

CHAPTER - III

SECTION - A

ULTRASONIC VELOCITIES AND
RELATED PARAMETERS STUDIES
IN SOME LIQUID CRYSTALS

SECTION - B

PRETRANSITIONAL EFFECTS AND
ORDER PARAMETERS STUDIES
IN SOME LIQUID CRYSTALS

CHAPTER - III

SECTION - A

ULTRASONIC VELOCITIES
AND RELATED PARAMETERS
STUDIES IN SOME
LIQUID CRYSTALS

The field of ultrasonics has grown enormously because of it's importance in providing a deep insight into the problems of basic physics. The importance of basic studies by ultrasonic waves is that of the structure of matter, and in that respect ultrasonic spectroscopy plays as an important role as X-ray spectroscopy. The study of ultrasonic wave propagation in the matter is well established and it provides an effective means to measure several physical constants. The rapid developments in the ultrasonic measurements techniques have brought important results which clearly demonstrate the capabilities of these measurements in the study of fundamental physical properties of the matter.

Since the discovery of the first liquid crystal by Reinitzer in 1888, ~~there~~ was little research in this field till three decades ago, when it was realized that their unique electrical, optical, electro-optical and thermal properties have emerged in many areas of applications, related to technology.

The simultaneous possession of liquid like (fluidity) and solid-like (molecular order) character in a single phase, made liquid crystals a fascinating field of research and hence attracted many researchers to this area of research. These researchers have been vigorously studying several physical aspects of liquid crystals behaviour, like the study of thermodynamical behaviour and the determination of the phase transition order, nuclear magnetic resonance, self diffusion

coefficient and the variation of order parameter at isotropic - mesomorphic phase transition refractive indices, Ultrasonic velocity and absorption and many other physical aspects.

9/ However ultrasonic studies in liquid crystals remain one of the important and fascinating properties as it provides a wealth of information about the phase transition mechanism which is having dependence on the structure. Moreover the measurements of ultrasonic velocity and density lead to the knowledge of important physical parameters like the adiabatic compressibility and molar sound velocity, which are of urgent importance in liquid crystals research. The knowledge of the thermal expansion coefficient and temperature coefficient of adiabatic compressibility lead to the precise analysis of the pretransitional effect in liquid crystals. Moreover with the help of thermal expansion coefficient data some of thermodynamical parameters e.g. specific heat, can be obtained easily, while they are difficult to be obtained by other thermodynamical methods.

In his ultrasonic studies on organic liquids, Rao concluded [1, 2] that the thermal coefficient of ultrasonic velocity is about three times the thermal coefficient of density i.e.

$$dV/V = 3 d\rho/\rho \dots\dots\dots (1)$$

Where V is the Ultrasonic Velocity and ρ is the density.

4/ However while testing the validity of his theory with the available experimental data, he found that few liquids depart

from this theory and water was one of them. Integrating and simplifying the above relation we get

$$V^{1/3}/S = K \dots\dots\dots(2)$$

where K is a constant; independent of temperature for any liquid. Multiplying by the molecular weight M the relation becomes

$$M/S (V)^{1/3} = R \dots\dots\dots(3)$$

Where R is known as Rao's Constant and M/S is the molar volume.

a/ For a particular liquid since M does not vary, Rao found that $M/S (V)^{1/3}$ is constant and named it as molar sound velocity. Different values for different bonds and linkages were proposed and it was found that the molar sound velocity R is an additive function of atoms and linkages and it is constitutive in nature to a large extent. His theory gave a closer agreement between the experimental and theoretical values. Langemann [3] independently proposed an alternative method of additivity of molar sound velocity, assigning certain values for different bonds instead of atoms and linkages as has been done by Rao. He established that his method gives better agreement between the computed and the experimental values of R. From extensive study of homologous series of organic liquids, Rao found that the molar sound velocity is analogous to other physical properties like parachor, Sander's viscosity constant and molar refraction.

Wada [4] developed another constant β given by

$$\beta = M/S (1/K_{ad})^{-1/7} \dots\dots\dots (4)$$

Where β is a constant over a wide range of temperatures and it has been termed as molar compressibility in analogy with molar sound velocity R . K_{ad} is the adiabatic compressibility given by the relation

$$K_{ad} = 1/S (V)^2 \dots\dots\dots (5)$$

Another advancement in the study of liquid state was made by Schaff [5] when he proposed that the Vander Waal's constant b and molecular radius could be computed at first approximation from the following expression

$$b = M/s [1-RT/MV^2 \{ (1+MV^2/3RT)^{1/2} -1 \}] \dots\dots\dots (6)$$

He formulated a relation which relates the ultrasonic velocity to the molecular weight, molecular volume and density

$$V^2 = rRT/ M-bS [M/3 (M-bS)] \dots\dots\dots (7)$$

Where R , S , M , V , T are respectively the gas constant, density, molecular weight, Ultrasonic velocity and temperature. He mentioned that the effective molecular radius r can be calculated from the relation

$$b = 16/3 \pi N r^3 \dots\dots\dots (8)$$

where N is Avogadro's number. He had tested the validity of his theory and obtained a good agreement between the theoretical and experimental results. It was found that the constant b is an additive function of atoms and linkages like some other constants. Schaff [6] has also derived the following relation

by which the available volume could be estimated

$$V_a = v (1 - V/V_0) \dots\dots\dots (9)$$

Where $V = 1600$ m/sec and v is the molar volume.

The Lennard-Jones Potential which is given by the relation

$$\phi(r) = [-A/r^6] + [D/r^n] \dots\dots\dots (10)$$

Where r denotes the intermolecular distance, n is the individual exponent describing the magnitude of the repulsive forces in the molecules and A and D are constants. The exponent n in the second term of the above relation is given by [7]

$$n = [(6v/V_a) - 13] \dots\dots\dots (11)$$

Assuming a spherical cage model. it has been assumed from the considerations of thermodynamics and statistical mechanics [8] that the free volume V_f is given by

$$V_f = (4\pi/3) K (R^3/v^2) (1/\alpha_T)^3 \beta_1^3 \dots\dots\dots (12)$$

Where v is the molar volume, α_T is the volume coefficient of expansion and K is the constant which depends on the geometry of packing.

LITERATURE SURVEY :

Due to the importance of Ultrasonic studies in liquid crystals as mentioned earlier, considerable interest has been shown by several researchers in studying Ultrasonic velocity and absorption in the isotropic phase and mesomorphic phase passing through the phase transition temperature. The density, besides being essential for the determination of order parameter, provides usefull information on the nature of the phase transition and pretransitional effects.

Gabrieli and Verdini [9] were the first researchers to investigate the ultrasonic velocity and absorption in p - azoxyanisole (PAA) and cholesteryl benzoate. They have observed anomalous behaviour of the variation of the ultrasonic velocity and adiabatic compressibility with temperature, while the velocity has shown a minimum, the adiabatic compressibility has shown a maximum at the isotropic - mesomorphic phase transition temperature in P-azoxyanisole, cholesteryl benzoate failed to show any anomaly at the isotropic-mesomorphic phase transition. Hoyer and Nolle [10] have reported their investigations of ultrasonic absorption on P-azoxyanisole in the frequency range of 0.5 MHz to 6 MHz. They have carried out their investigations on cholesteryl benzoate in an inert atmosphere to avoid any contamination of the sample as it is susceptible to oxidation. An abrupt maximum change in velocity and absorption were observed at the isotropic mesomorphic phase transition in both liquid crystals. They have related these anomalies to the pretransitional effect and interpreted the results in the light of the heterophase fluctuation theory [11]. Zvera and Kapustin [12] have investigated the ultrasonic properties in poly mesomorphic cholesteryl caparate which exhibits a cholesteric and smectic phases. They have observed anomalous behaviour with a minimum in velocity and a maximum in absorption at the isotropic-cholesteric phase transition and no anomalous changes at the cholesteric-smectic phase

transition. They have attributed this anomaly to the structural relaxation process. Kapustin and Bykova [13] have studied the ultrasonic properties in polymesomorphic P-n-Octyloxybenzoic acid and P-n-heptyloxybenzoic acid which exhibit both nematic and smetic phases. A sharp decrease in velocity at the isotropic-nematic phase transition was observed whereas a slight change was observed at the nematic-smetic phase transition. They have attributed the anomaly at phase transition to the molecular order as the temperature is lowered from the disordered isotropic state to the more ordered mesomorphic state. Kapustin [14] independently reported anomalous behaviour in ultrasonic velocity, related parameters and absorption at isotropic-mesomorphic phase transition in different types of liquid crystals and attempted to interperate the axess absorption at phase transition on the basis of thermodynamic theory of critical phenomena proposed by Semenchikov [15]. He related the maximum adiabatic compresibility at phase transition to the presence of stochastic fluctuations and hence concluded that the system has a lower stability at isotropic-mesomorphic phase transition. Kapustin and Martyanova [16] have attempted to interperate the velocity minimum at phase transition in P-azoxyanisol (PAA) and P-azoxyphenetol (PAP) on the basis of the molecular statistical theory proposed by Maier and Saupe [17-19]. Kartha and Padmini [20, 21] have studied density, ultrasonic velocity and related

parameters and ultrasonic absorption in Cholesteryl acetate, cholesteryl benzoates and cholesteryl Stearate. They have reported anomalies at the cholesteric- isotropic phase transition in all these liquid crystals. They have analysed the velocity results in the light of Frenkel's theory [12] and absorption results in the light of Fixman's theory [22]. Otia and Padmini [23] have measured density, and ultrasonic velocity in MBBA, EPAPU and estimated the temperature variation of order parameter S in the nematic phase. They have as well [24] studied ultrasonic velocity and related parameters in cholesteryl propionate, cholesteryl laurate, and cholesteryl myristate at the isotropic-cholesteric and cholesteric-smectic phase transition. Anomalies in the ultrasonic velocity and other related parameters were observed at the phase transition temperature. Kor and Pandey [25] have studied the ultrasonic behaviour in cholesteryl nonanoate, cholesteryl decanoate and cholesteryl linolate. Kawamura et al [26] have investigated the ultrasonic velocity and absorption in MBBA and EBBA as a function of temperature and frequency. A sharp maximum was observed in the attenuation coefficient and a sharp minimum in the ultrasonic velocity. The anomalous behaviour was explained in the light of Landau - Khalatnikov's theory [27]. Langunov et al [28] measured the ultrasonic velocity and absorption in p-anisal amino azobenzene in the nematic phase in the frequency range of 1 MHz to 60 MHz.

Bhattacharya [29] et al have observed strong anomalies in the velocity and attenuation at the vicinity of nematic-smectic A phase transition in TBBA. This group of researchers have carried out extensive investigations on liquid crystals exhibiting $S_A - S_B$ and $S_A - S_B$ phase transitions. George et al [30, 31] have studied ultrasonic velocity, density in nematic and polymeric liquid crystals. The pretransitional effect was investigated in the thermal expansion coefficient and temperature coefficient of adiabatic compressibility and explained their results in the light of de Gennes theory generalized by Bendler[32]. The ultrasonic velocities at isotropic-nematic, $N-S_A$, S_A , S_B , S_A-S_C , $N-S$, S_C-S_G and S_B-S_G phase transitions were extensively investigated by Rao and Pissipati [33-35]. They have reported the ultrasonic velocity and related parameters and observed anomalous behaviour in all these phase transitions. They have also studied ultrasonic velocity and density in p-n heptyloxybenzylidene-p-n-octylaniline and (p-n-hexyloxybenzylidene) phenylazoaniline polymeric liquid crystals. They have shown that $I-S_A$, S_A-S_C , S_B-S_C phase transitions are all of first order [36, 37]. Dhake, K.P. et al [38-40] recently have measured the ultrasonic velocity in p-n-octyloxy benzylidene- p- phenetidine (OBP). They have analyzed the pretransitional effects and interpreted their results in the light of Bendler's theory [32]. They have also studied the ultrasonic velocity and density in p- methoxy- p-

propanoyloxy benzoate (PMPAB) AND p-(p-methoxy benzylidene) amino phenylacetate (MBAPA). They have compared their results with X-ray data and analyzed the results on the basis of Maier and saupe theory [17-19]. George[41,42] has reported the ultrasonic studies and pretransitional effects analysis in cyanobiphenyl in the isotropic- nematic phase transition. Malikarjuna Rao and Srinivas Rao [41,42] reported the ultrasonic velocity and pretransitional effect studies in 60CB, 70CB and 4-cyano-4'-n-heptylbiphenyl. They have interpreted their results on the basis of Frenkel theory [11].

Results:

The above survey indicates that a good amount of research has been done in the study of ultrasonic velocity and density in different liquid crystals. However, very few liquid crystals have been investigated collectively and systematically as a group of one liquid crystal series. The survey indicates also that the studies on adiabatic compressibility, molar sound velocity and Wada's constant are scares. Therefore in the present investigations the author has chosen series of liquid crystals viz. I p(p'-n alkyloxybenzoyloxy)nitrophenol and p(p'-n alkyloxybenzoyloxy) benzaldehyde.

Three and two consecutive members from the first and second series were selected respectively, so that the variation of chain length and the substituent groups effect on the physical properties is studied systematically. The liquid crystals

which are the subject of the present investigation are

1. p(p'-n pentyloxybenzoyloxy)nitrophenol (PBNP).
2. p(p'-n hexyloxybenzoyloxy) nitrophenol (H6BNP).
- * 3. p(p'-n heptyloxybenzoyloxy)nitrophenol (H7BNP).
- * 4. p(p'-n heptyloxybenzoyloxy)benzaldehyde (HBB).
5. p(p'-n octyloxybenzoyloxy)benzaldehyde (OBB).

monotropic

nematic

smectic

enantiotropic

How?
How?

All the liquid crystals mentioned above are henceforth represented in the abbreviated forms as given in the brackets.

The first three liquid crystals are monotropic. PBNP, H6BNP are nematic while H7BNP is smectic. HBB, OBB are enantiotropic

liquid crystals and both of them are nematics. The transition temperatures are measured with the help of Leitz polarizing microscope and are given in table A. The ultrasonic velocity measurements were carried out by employing double crystal fixed path interferometer at 2 MHz frequency. The density measurements were carried out using a dilatometer specially developed for this purpose. The details of the experimental set up are given in chapter II. The ultrasonic velocity (V) and density (S) are measured in all the liquid crystals at around 10°C above and below the isotropic-mesomorphic transition temperatures i.e. in around 20°C temperature range in which the isotropic and mesomorphic phases are exhibited. Special care was taken at the vicinity of the isotropic-mesomorphic transition temperature. The temperature of the oil bath in which the ultrasonic cell is immersed is controlled to the accuracy of

$\pm 0.02^\circ\text{C}$. The transition temperatures of the liquid crystals studied and the molecular weights are given in Table A. All the measurements have been taken while cooling.

The Tables A1 through A5 represent the actual measurements of velocity (V) density (ρ) of PBNP, H6BNP, H7BNP, HBB and OBB at different temperatures. The parameters viz. adiabatic compressibility (k_{ad}), molar sound velocity (R) and Wada's constant (β) are included in the same tables. Figures A1 through A20 represent the ultrasonic velocity (V), density (ρ), adiabatic compressibility (k_{ad}), molar sound velocity (R) and the Wada's constant β for the five liquid crystals viz PBNP, H6BNP, H7BNP, HBB and OBB respectively.

The order parameter (S) studies and the pretransitional studies viz. thermal expansion coefficient (α_T) and temperature coefficient of adiabatic compressibility, the available volume and Lennard-Jone's potential are presented and discussed in section B of this chapter.

Temperature Variation of Ultrasonic Velocity (V) and Density (ρ) in PBNP:

Figure A1 represents the temperature variation of ultrasonic velocity and density respectively in the monotropic nematic liquid crystal PBNP. It is indicated that the velocity exhibits an anomalous behaviour at the isotropic-nematic phase transition temperature, while it varies linearly in the isotropic and nematic phases away from the transition. The velocity shows a

dip of 27 m/s at phase transition . The density shows a sharp jump of 2.0×10^{-3} gm/cm³ at the vicinity of the phase transition while it varies linearly in the isotropic and nematic phases.

Temperature Variation of Adiabatic Compressibility (k_{ad}),

Molar Sound Velocity (R) and Wada's Constant (β) in PBNP :

Figures A3 and A4 represent the variation of adiabatic compressibility, molar sound velocity and Wada's constant respectively. The Figure shows that the adiabatic compressibility varies linearly in both the phases while the molar sound

9. velocity (R) shows a remarkable linear variation. At the isotropic -nematic transition the adiabatic compressibility is

indicated by a step maximum of 46.08×10^{12} cm²/dyne, while the molar sound velocity is indicated by a step minimum of 3172.11.

7. A glance at the figures show that Wada's Constant varies also with remarkable linearity with temperature and exhibit a dip of 165.447 at the isotropic-nematic phase transition.

Temperature Variation of Ultrasonic Velocity (V) Density (ρ) in H6BNP:

Figures A5 and A6 represent the variation of ultrasonic velocity (V) and density (ρ) in the monotropic nematic liquid crystal H6BNP. It is clear from the figures that the ultrasonic velocity and density variation with temperature show anomalous behaviour at the isotropic-nematic phase transition while both physical properties vary linearly away from phase transition. The ultrasonic velocity shows a sharp dip of 22 m/s, the density shows a sharp dip of 2.1×10^{-3} g/cm³.

Temperature Variation of Adiabatic Compressibility (K_{ad}),

Molar Sound Velocity (R) and Wada Constant (Beta) in H6BNP:

Figures A7 and A8 represent the temperature variation of adiabatic compressibility, molar sound velocity and Wada constant respectively. A glance at the figures reveal that all the three parameters show an anomalous behaviour at the isotropic-mesomorphic phase transition. However, the variation with temperature is linear in the isotropic and nematic phases. The adiabatic compressibility is indicated by a sharp maximum of $48.10 \times 10^{12} \text{ cm}^2/\text{dyne}$ while the molar sound velocity is indicated by a sharp minimum of 3367.88 at the isotropic-nematic phase transition. The results show that Wada's constant shows a sudden minimum of 175.185.

Temperature Variation of Ultrasonic Velocity (V) and Density (S) in H7BNP :

Figures A9 and A10 represent the temperature variation of ultrasonic velocity and density in the monotropic smectic liquid crystal H7BNP. It is clear from the figures that the ultrasonic velocity shows a linear variation in both phases, but behaves anomalously at the isotropic-smectic phase transition at which a step minimum of 19 m/s is exhibited. The density shows a linear variation in the isotropic and smectic phases. It is observed that the density shows a sharp dip of $2.3 \times 10^{-3} \text{ g/cm}^3$ at the isotropic-smectic phase transition.

Temperature Variation of Adiabatic Compressibility (K_{ad}),
Molar Sound Velocity (R) and Wada's constant in H7BNP:

Figures A11 and A12 represent the temperature variation of adiabatic compressibility molar sound velocity and Wada's constant respectively. It can be observed that the three parameters show anomalous behaviour at the isotropic-smectic phase transition while they vary linearly in the isotropic and smectic phases away from the transition. The adiabatic compressibility shows a sharp maximum of $49.06 \times 10^{12} \text{ cm}^2/\text{dyne}$ and the molar sound velocity a sharp minimum of the value 3512.36. The Wada's constant exhibits a minimum of 182.638 at the isotropic-smectic phase transition.

Temperature Variation of Ultrasonic Velocity (V) and Density
(ρ) in HBB:

9. Figures A13 and A14 represent the variation of ultrasonic velocity and density in the enantiotropic nematic liquid crystal HBB. An examination of the figure reveals that the ultrasonic velocity shows a remarkable linear variation in the isotropic phase while it shows a linear variation in the nematic phase. However the ultrasonic velocity show anomalous behaviour at phase transition as it shows a sharp minimum of 25 m/s. The density exhibits a linear variation in the isotropic and smectic phases but shows a jump of $3.2 \times 10^{-3} \text{ g/cm}^3$ at the isotropic - nematic phase transition.

Temperature Variation of Adiabatic Compressibility (K_{ad}),
Molar Sound Velocity (R) and Wada's Constant in HBB:

Figures A15 and A16 represent the variation of adiabatic compressibility, molar sound velocity and the Wada's constant variation with temperature respectively. An examination of the figures reveal that the three parameters vary with a remarkable linearity with temperature away from the phase transition but behave anomalously at phase transition. The adiabatic compressibility shows a step maximum of $55.32 \times 10^{12} \text{ cm}^2/\text{dyne}$ while a step minimum of 3723.93 is exhibited by the molar sound velocity. The Wada's constant exhibit a sharp minimum of 189.469 at the isotropic nematic phase transition.

Temperature Variation of Ultrasonic Velocity (V) and Density (S) in OBB :

Figures A17 and A18 represent the temperature variation of ultrasonic velocity and density in the enantiotropic nematic liquid crystal OBB. An examination of the figures reveal that the velocity exhibits an anomalous behaviour at the isotropic-nematic phase transition. The velocity shows a linear variation in the isotropic and nematic phases away from the transition and exhibits a sharp minimum of 15 m/sec at phase transition, the density also shows a linear variation in both the phases and exhibits a dip of $3.4 \times 10^{-3} \text{ g/cm}^3$.

Temperature Variation at Adiabatic Compressibility, Molar Sound Velocity (A) and Wada's Constant (B) in OBB :

Figures A19 and A20 represent the temperature variation of adiabatic compressibility, molar sound velocity and Wada's constant respectively in the enantiotropic nematic liquid crystal OBB. It can be seen from the figure that the three parameters show anomalous behaviour at the Isotropic - nematic phase transition while they vary linearly in the isotropic and nematic phase away from the transition. The adiabatic compressibility shows a sharp maximum of the value of $57.34 \times 10^{12} \text{ cm}^2/\text{dyne}$, the molar sound velocity shows a sharp minimum of 3916.31. The Wada's constant behaves in the same manner and shows a minimum of 200.36 at the isotropic-nematic phase transition.

DISCUSSION :

The above results firmly indicate that ultrasonic velocity and related parameters such as adiabatic compressibility molar sound velocity and Wada's constant are all structure dependent parameters. Further these parameters are also related to the intermolecular attraction, molecular association and the degree of molecular order. The molecules in the mesophase are all arranged with their long axis parallel to a preferred direction, and the degree of molecular order increases from nematic to smectic while in the isotropic phase the molecules are arranged randomly and there is no such orderliness, and the

degree of molecular order is zero. Maier and Saupe [17-19] have developed molecular statistical theory of nematic phase which is based on an average internal field of the Weiss molecular field in ferromagnetism. They have assumed that the dipole-dipole part of the pure dispersion forces are predominantly responsible for the formation of nematics. They have defined the order parameter (S) characterising the nematic phase as the second order legendre polynomial,

$$S = 1/2 (3 \cos^2 \theta - 1)$$

where θ is the angle between the long axis of the molecule and the axis of preferred orientation which coincides with the symmetry axis of uniformly oriented nematic.

An examination of the figures reveals that the ultrasonic velocity and related parameters exhibit an anomalous behaviour at the isotropic-meromorphic phase transition. The figures indicate also that with the decrease in temperature, initially the velocity increases linearly and afterwards it becomes mon-linear with further decrease of temperature, following the normal behaviour of liquids. This increase in ultrasonic velocity is explained as the decrease in the mean distance between the molecules thereby increasing the potential energy interaction between them. The increase in velocity with the decreasing temperature and hence the increase in molecular interaction is accompanied by a decrease in the adiabatic compressibility. However at the isotropic nematic phase

transition the random molecular arrangement in the isotropic phase changes over to an ordered arrangement and at the vicinity of phase transition the isotropic phase exists in the pretransitional state, thus leading to vigorous heterophase fluctuations. These fluctuations enhance the compressibility of the medium enormously and hence the decrease of ultrasonic velocity is observed. The detailed analysis and the estimation of the numerical values of the order parameter (S), the pretransitional effect in thermal expansion coefficient (α_T) the temperature coefficient of adiabatic compressibility (B_T) and the Lennard Jones potential are included in section B of this chapter. The x-ray investigations on MBBA explains the variation of interatomic distance and specific volume with temperature in the nematic phase. X-ray studies of de Vries [23-24] on bis-(4'-n-octyloxybenzal)-2-chloro-4-phenylenediamine has shown that in the nematic phase some of the molecules are arranged in organised groups. These groups are called cybotactic groups. At lower temperatures the large majority of the molecules are arranged in these groups appear to be fairly rigid. At higher temperatures the groups become less prominent but they do not disappear completely. These investigations suggest that, in the mesophase at lower temperature, the intermolecular attractions are strong enough to make the cybotactic groups more rigid. With the increase in temperature these attractions become weakened and suddenly at

*

the phase transition the groups must have been disrupted. The detailed numerical estimation of the repulsive force is estimated from Lennard - Jones potential and included in section B of this chapter.

Our present investigations on ultrasonic velocity and related parameters confirm the findings of X-ray studies. With increase of temperature, the ultrasonic velocity decreases and adiabatic compressibility increases, indicating the weakening of the interplanar, interterminal and intermolecular attraction between the molecules and at the isotropic-mesomorphic phase transition the breaking of the cybotactic groups into disordered liquid is depicted as a dip in the ultrasonic velocity and a maximum in the adiabatic compressibility. The specific volume jumps and the thermal expansion coefficient, the temperature coefficient of adiabatic compressibility confirm the first order isotropic-nematic transitions of the all the liquid crystals studied. However, the detailed and numerical estimations of these parameters is included in the next section.

CHAPTER - III

SECTION - B

PRETRANSITIONAL EFFECTS

AND ORDER PARAMETERS

STUDIES IN SOME

LIQUID CRYSTALS

In recent years, considerable interest has been shown to study the behaviour of physical properties of the isotropic mesomorphic phase transition/ among them ultrasonic velocity and density play an important role in characterising the phase transition. The advantage of ultrasonic studies over the other studies is that they provide information about the static & dynamic properties of the system, while the ultrasonic velocities provide precise information about the equilibrium adiabatic properties ultrasonic attenuation provides direct information about the dynamic behaviour and from the attenuation studies as a function of frequency and temperature, much can be understood about relaxational mechanisms responsible for ultrasonic attenuations. Liquid crystalline phase transitions are first order with latent heats of 0.1 to 0.7 kcal/mole for nematics and cholesterics and 1-3 kcal/mole for smectics. Maier and Saupe have developed a molecular statical theory of nematic phase which is based on an average internal field of the Weiss molecular field in ferromagnetism. They have assumed that the dipole-dipole part of the pure dispersion forces are predominantly responsible for the formation of nematics. They have defined an order parameter & characterising the nematic phase as

$$S = \frac{1}{2} (3\cos^2\theta - 1)$$

Where θ is the angle between the long axis of a molecule and the axis of preferred orientation which coincides with the

summetry axis in uniformly oriented nematic phase. Here a brief review of some of the important theories of phase transition related to liquid crystals are given.

A- Landau Theory of Phase Transition :

Landau and Khalantikov [27] were the first to develop a dynamic theory and to discuss ultrasonic attenuation and dispersion in the vicinity of a λ transition theory on the basis of main field of Bragg and Williams. The theory which is particularly applicable to second order phase transition [2], involves a power series expansion of the free energy near the transition point in terms of the order parameter

$$\phi = \phi_0 + \alpha n + An^2 + Bn^3 + Cn^4 \dots \dots \dots (1)$$

The continuous nature of the change of state at the phase transition permit this expansion to be made. The coefficients ϕ_0 , α , A , B , C , \dots are assumed to be functions of pressure P and the temperature (T). On the basis of symmetry arguments of second order phase transition. Landau sets $\alpha = \beta = 0$, so the relation reduces to

$$\phi = \phi_0 + An^2 + Cn^4 + \dots \dots \dots (2)$$

The equilibrium value of n is determined from the condition

$$\begin{aligned} \partial\phi/\partial n &= 0 & n=0 \text{ when } T > T_c, \\ & & n \neq 0 \text{ when } T < T_c. \end{aligned}$$

B. Landau - de Genne's Theory of Phase Transition :

An important advancement has been made towards the understanding of the mechanism of phase transition by Landau [45] when he proposed a theory describing the functional dependence of

the free-energy density on the order parameter and its spatial derivatives near a second order phase transition. Landau has speculated that near second order phase transition, free energy density function can be expanded as a power series in the order parameter and its spatial derivatives, with temperature dependant coefficients and sufficiently close to the transition only the first few terms of the series are important. Despite certain shortcomings, Landau's theory of phase transition has proved to be as good as mean field theory in providing a semiquantative description of the specific heat, the order parameter and the entropy in the vicinity of a second-order phase transition. Although originally intended as a theory of second order phase transition, de Gennes [46] was the first to successfully apply the theory to the first order liquid crystal phase transitions.

Following Landau expression, free-energy density in the vicinity of phase transitions, can be written as

$$F(n, P, T) = F_0 + 1/2 A(P, T) n^2 - 1/3 B(P, T) n^3 + 1/4 C(P, T) n^4 + \dots \quad (3)$$

for a second order parameter $B=0$,

$$F = F_0 + 1/2 A(P, T) n^2 + 1/4 C(P, T) n^4 \dots \dots \dots (4)$$

Where A and C depend upon the temperature and pressure. The order parameter satisfies the condition that its equilibrium value is zero for $T > T_c$ and non-zero for $T < T_c$.

Landau assumed further that near T_c , the coefficient C is a slowly varying function of T, compared to A(T). This constant

$A(T)$ must be positive for $T > T_c$ in order that $n = 0$ be a minimum for $F(n, T)$, and negative for $T < T_c$ which implies that $A(T=T_c)$ must be zero and in the neighbourhood of T_c , $A(T)$ can be approximated by

$$A(T) = a (T-T_c)$$

Where 'a' is a constant. The free-energy density expression can now be re-written as

$$F = F_0(T) + 1/2 a(T-T_c)n^2 + 1/4 C n^4 ; \quad a, c > 0 \quad \dots\dots\dots (5)$$

If the spacial variation of the order parameter are taken into account, n can be replaced by $n(r)$; and the interaction terms $r[n(r), T]$ should be included in the free-energy expression:

$$F[n(r), T] + r[n(r), T] = F_0(T) + a/2 (T-T_c)n^2(r) + 1/4 C n^4(r) + 1/2D [\nabla n(r)]^2 \quad \dots\dots\dots (6)$$

The expression for the free-energy density can be generalised to include the special symmetry properties of cholesteric liquid crystals since cholesteric order is indistinguishable from nematic order on a microscopic scale. However, the spacial variations of the local order in cholesteric liquid crystals exhibits always a helical ordering on a macroscopic scale compared to molecular dimensions.

C. Bendler's Modification of de Gennes' Theory :

de Gennes theory of pretransition effects in the isotropic liquid was generalized by Bendler [32]. The Landau model of de Gennes [45] is based on an expression of free-energy in terms of an order parameter and gradients in the order parameter. The

same approach is made by Bendler, but the difference is that while de Gennes has defined the order parameters in terms of diamagnetic anisotropy of the system, Bendler identified the order parameter from a spherical harmonic expansion a pre-averaged molecular probability density. This theory allows for number density fluctuations in addition to the orientational ones, which enables the observed anomalies in compressibility and thermal expansion:

The anomalies in thermal expansion coefficient (α_T) and temperature coefficient of adiabatic compressibility (B_T) are explained by Bendler [32] who has suggested that there is a local linear coupling of order density. consequently the order fluctuations which becomes large near the transition produce an excess internal pressure and with enhanced compressibility result in a more rapid contraction of the fluid. It is assumed that the expansion anomaly is the result of compressibility anomaly; with this approximation Bendler has given the thermal expansion and compressibility anomalies as

$$\beta_T = B (T - T^*)^{-\tau} \dots\dots\dots (7)$$

$$\alpha_T = A (T - T^*)^{-\tau} \dots\dots\dots (8)$$

Where A and B are constants and independent of temperature in the vicinity of transition $T = (T_c - 1)$ is the pseudo critical temperature and n is the critical exponential.

Bendler's theory predicts that in the isotropic phase above the clearing temperature T_c , coefficient of thermal expansion

should have the form

$$\chi_T = \chi_0 + A (T-T_c)^{-x} \dots\dots\dots (9)$$

where χ_0 is the normal background term which is unaffected by the order fluctuations. He has given the following expression for compressibility anomaly as

$$B_T = B_0 + B (T-T_c)^{-x} \dots\dots\dots (10)$$

Where B_0 is the normal background term unaffected by fluctuations.

D. Thermodynamical Behaviour of Liquid Crystals at Phase Transition :-

Considering a spacially uniform system in which the order parameter value is spacially invariant, the expression for free-energy density can be given as

$$F(S, T) = F_0(T) + 3a/4 (T-T_c^*) S^2 + 1/4 B S^3 + 9/16 C S^4 \dots\dots (11)$$

The equilibrium value of the order parameter, $\langle S \rangle$, is equal to the value of S which minimises F of each T . Hence differentiating the above equation with respect to S and set the results equal to zero for $S = \langle S \rangle$, One obtains for high temperature isotropic phase $\langle S \rangle = 0$ and the order parameter value at the low temperature phase at $T = T_c$ is obtained as

$$\langle S \rangle_c = -2/9 B/C, \quad B < 0$$

The entropy per molecule s , in the nematic phase can be obtained

$$s = -1/N (\partial F^0(T)/\partial T) = s_0 - 3a/4N \langle S \rangle^2 \dots\dots\dots (12)$$

and transition entropy per molecule, Δs , as

$$\Delta s = -1/27 \cdot aB^2/NC^2 \dots\dots\dots (13)$$

The system transforms from the high temperature phase $\langle S \rangle = 0$ to the low temperature phase $\langle S \rangle \neq 0$ at a temperature

$$T_c = T_c^* + B^2/27ac \dots\dots\dots (14)$$

These equations are usually used as the means by which the phenomenological parameter a , B and C for any liquid crystal are determined from the experimental values of $\langle S \rangle_c$, ΔS and $(T_c - T_c^*)$.

E. Maier-Saupe Theory of Nematic Liquid Crystals :

Maier-Saupe have proposed an important theory of nematic phase based on the internal molecular field postulate closely ✓ analogous to that suggested by Weiss in explaining the phenomenon in of ferromagnetism. Maier and saupe have assumed that the molecules in the nematic phase are cylindrically symmetric and so the pairwise intermolecular potential may be written as

$$U_{12}(r; \theta_1, \phi_1; \theta_2, \phi_2) = 4\pi \sum_{L_1, L_2, n} u_{L_1 L_2 n}(r) Y_{L_1, n}(\theta_1, \phi_1) Y_{L_2, -n}(\theta_2, \phi_2) \dots (15)$$

Where $Y_{L, n}(\theta, \phi)$ is the n th component of the L th spherical harmonic. The orientational energy of the single molecule resulting from its interaction with all other molecules is obtained by averaging over the coordinates of all the molecules. From this orientational energy of a single molecule, the orientational order parameter S characterising the mesophase is given by

$$S = \frac{\int [1/2 \{3 \cos^2 \theta - 1\} \exp\{-u(\cos \theta)/KT\} d \cos \theta]}{\int \exp\{-u(\cos \theta)/KT\} d \cos \theta} \dots\dots\dots (16)$$

Maier - Saupe theory implicitly ignores all but these terms with $L_1 = L_2 = 2$. in the expansion of the intermolecular potential. The intermolecular vector is then assumed to be uniformly distributed within the mesophase and the molecular field.

Maier and Saupe's theory has led to a universal curve for S as a function of $TV^2/T_c V_c^2$, Where T, V are the absolute temperature and molar volume in the nematic phase, T_c, V_c the corresponding values at the nematic- isotropic transition point, and $S_k = 0.44$ for all the nematic liquid crystals. Although the predicted variation agrees with the experimental data, significant deviations from the universal curve has been observed in many cases.

Order Parameter :

Chandrasekhar and Co-workers proposed an elementary theory of the birefringence of the nematic state with the important postulation that the intermolecular interactions are predominantly of the dipole-dipole type. While developing the theory they have taken into account not only the dipole - dipole interactions but also the anisotropic dispersion, induction and repulsion forces all of which definitely contribute to the orientational potential energy. They have obtained for the orientational potential energy of a molecule as :

$$U = -C_1(1-C_2\theta^2) \dots\dots\dots (17)$$

Where C_1 and C_2 are Constants so that

$$du/d\theta = 2C_1 C_2 \theta, \quad \text{or}$$

$$du/d\theta \propto \theta$$

Thus the molecules may be expected to execute rotational oscillations or librations about the mean orientation. Chandrasekhar and co-workers supposed that the librations can be treated in terms of an Einstein model and assumed the well-known relation

$$H \propto S^{-1/6} B^{-1/2} \dots \dots \dots (18)$$

Where H is the Einstein Characteristic temperature, S the density and B the adiabatic compressibility.

Since $B = 1/SV^2$

Where V is the ultrasonic velocity in the liquid crystal Cruickshank [47,48] has shown that when $T \gg H$, the mean square libration amplitude is given by :

$$\overline{\theta^2} = h^2 T / 4\pi I k H^2$$

where T is the absolute temperature h is the Plank's constant, I is the moment of inertia of molecule and K is Boltzmann's Constant. There for $\overline{\theta^2}$ can be written as

$$\overline{\theta^2} \propto T S^{-2/3} V^{-2} \dots \dots \dots (19)$$

$$\overline{\theta^2} = B T S^{-2/3} V^{-2}$$

$$\theta_{rms} = (\overline{\theta^2})^{1/2} \dots \dots \dots (20)$$

Where B is a constant and Chatelain [49] and Maier and Saupe [17-19] have expressed the degree of orientation of the molecules in terms of a factor

$$S = 1/2 (3\cos^2\theta - 1) \quad \checkmark$$

Where S is the order parameter and θ is the angle between the long axis of the parallel molecules with a preferred direction. It can readily be shown that for rotational oscillations :

$$S = \frac{1}{2} [\cos^2 (\sqrt{2} \theta_{rms}) + \cos (\sqrt{2} \theta_{rms})] \text{ When } \theta_{rms} = (\overline{\theta^2})^{1/2} \dots\dots\dots (21)$$

Literature Suvey :

Considerable work has been done by different workers to study the pretransitional effects in isotropic phase of nematic and cholesteric liquid crystals. A brief review of the important investigations is given here. Stinson and Litster [50] have investigated the magnetic birefringence in the isotropic phase of the nematic liquid crystal p-methoxy benzyldene p-n butylaniline (MBBA) as a function of temperature. They have measured the intensity and spectrum of light scattered by anisotropic fluctuations in the dielectric constant and observed a divergence in critical slowing of the fluctuations in order as the isotropic-mesomorphic phase transition was approached. They have explained their results by Landau- de gennes theory of phase transition [45,46]. Yang [51] studied Rayleigh scattering in a cholesteric phase in 2-(2-ethoxy) ethoxy ethyl carbonate. They have observed that both the Rayleighs width & its inverse intensity show $(T-T^*)$ dependence, where T^* is the second order phase transition temperature. They have interpreted their results on the model suggested by de Gennes [46,52] in their isotropic phase. Chu, Bak and Lin

[53] have measured angular dependence of polarised I_{11} and depolarised I_1 scattered light intensity by fluctuations of the order parameter Q near the isotropic nematic phase transtion of MBBA. They have found that the intensities $I_{11,0}$ and $I_{1,0}$ are proportional to ϵ^r where $r = 1$ and $T_c - T^* = 1.00 \pm 0.5^\circ\text{C}$, agreeing with de gennes theory. Chung and Meyer [54] have investigated the optical rotation in the isotropic phase of cholestiric liquid crystals near the isotropic - cholestric phase transition and observed a sharp increase in the rotatory power. They have interpreted their results on the basis of Landau - de gennes theory and predicted $(T-T^*)^{-1/2}$ temperature dependence and obtained a good agreement with experimental results in the pretransitional region.

Chung, Meyer and Gruler [55] have measured the nematic elastic constants namely, play and bend constant of a polymesomorphic (CBOOA) as a function of temperature. They have observed that the bend constant diverges near the nematic - smectic A phase transition with the temperature dependance as predicted by de Gennes. Several other workers have reported their investigations on the nematic smectic A transitions [56,58]. Otia and Padmini [59] have investigated the pretransitional effects in MBBA, EPAPU, (nematic), cholesteryl proplonate (cholesteric) cholesteryl laurate and cholesteryl myristate (polymesimophic) at the isotropic-nematic, and cholesteric-smectic, the isortopic-cholestric-smectic. A phase transitions, by study-

ing the parameter thermal expansions and isothermal compressibilities. The anomalies in thermal expansion and isothermal compressibilities were interpreted in the light of Landau- de Genne's theory generalised by Bendler. They have also estimated the order parameter variation with temperature from the ultrasonic velocity data. Kartha and Padmini [60] have studied the order parameter variation with temperature in mixed liquid crystals, from the ultrasonic velocity. George and Padmini have observed pretransitional effects in a monotropic nematic liquid crystal p-anisal - p - phenetidine (pApP), and a polymeric liquid crystal, p-p- decyloxy benzoyl-p-cresol (DBC) which exhibits nematic and smectic A phases. They discussed the pre transitional effects in specific volume and adiabatic compressibility on the basis of de Gennes theory generalized by Bendler and they estimated the critical exponents. The temperature variation of the order parameter was also estimated [31]. George et al [30] and George independently [41,42] have studied the pretransitional effect and estimated the critical exponent in the nematic - isotropic phase transition.

Results and Discussion:

In this section an attempt has been made by the author to investigate the pretransitional effects by Bendler in the parameters, thermal expansion coefficient (α_T) and the temperature coefficient of adiabatic compressibility (B_T) in

the liquid crystals PBNP, H6BNP and OBB, employing de Gennes theory generalised by Bendler. The experimental thermal expansion coefficient is calculated from the relation

$$\alpha = (1/V_n) (dV/dT) \dots\dots\dots (22)$$

where V_n is the average specific volume for the temperature difference of ΔT and ΔV is the specific volume across the temperature at ΔT . The temperature coefficient of adiabatic compressibility (β) is calculated from the relation

$$\beta = 1/K_o (dK_{ad}/dT) \dots\dots\dots (23)$$

where K_o is the adiabatic compressibility where the maximum occurs.

The author has made an attempt also to estimate the values of the order parameter from the specific volume measurements (density) of all the liquid crystals studied. The volume jumps (ΔV_k) occurring at the isotropic-mesomorphic transition is estimated. The ratios $\Delta V_k / V_{k,n}$ are estimated for all the liquid crystals studied from Mayer & Saupe theoretical curve between $\Delta V_k / V_{k,n}$ and S_k (Figure B) corresponding values of S_k are read. The values of $A/KT_k V_{k,n}$ are also estimated from the same curve. Using relation (21) and taking the value of the order parameter at phase transition S_k , the value of θ_{rm} is computed. Using the value of θ^2 and the values of ultrasonic velocity and density at the phase transition temperature in equation (19), the value of the constant B is calculated. Assuming that this constant does not vary much with temperature the values of S at

various temperatures are estimated with the help of ultrasonic velocity and density data. From the values of θ^2, θ_{rms} and hence the order parameter S values are estimated at various temperatures in the nematic phase. Bendler has predicted that the number density fluctuations which are governed by order fluctuations will vary with temperature above the nematic transition as

$$\Delta s^2 \approx (T - T^*)^{-r} \dots\dots\dots (24)$$

where T^* is the pseudo-critical temperature of the nematic ordering and r is the component determining the growth of order fluctuations. Light scattering and magnetic birefringence studies have shown that r is very near to unity and $(T - T^*) = 1$ for MBBA. Bendler has suggested that these density fluctuations produce an increase in isothermal compressibility which can be expressed as

$$K_T = K_0 + C(T - T^*)^{-r} \dots\dots\dots (25)$$

where K_T is the isothermal compressibility. He also assumed that the compressibility anomaly is the sole origin of the expansion anomaly which can be expressed as

$$\alpha_T = \alpha_0 + A(T - T^*)^{-r} \dots\dots\dots (26)$$

From

$$dK_T/dT = -Cr(T - T^*)^{-r-1} \dots\dots\dots (27)$$

or $1/K_T^0 = dK_T/dT = -C(T - T^*)^{-r-1} \dots\dots\dots (28)$

where K_T^0 is taken at the temperature where the compressibility maximum occurs and C' is another constant. The relation between

K and K_{ad} can be written as $K = r_{sp} K_{ad}$ where r_{sp} is the ratio of specific heats. Since the pretransitional effects observed in K_T , C_p and r are similar in nature to that of K_{ad} , it can be reasonably assumed that the nature of the variation of $(1/K_{ad}^0) dK_{ad}/dT$ must be analogous to that of $(1/K_T^0) dK_T/dT$. Hence,

$$-C' (T-T^*)^{-r'-1} \sim 1/K_{ad}^0 dK_{ad}/dT \dots\dots\dots (29)$$

Or

$$B_T = B_0 + B(T-T^*)^{-r'} \dots\dots\dots (30)$$

where B_0 is constant away from the transition point and $(r'=r+1)$
A study of the experimental results (Figure B1 through B10 of thermal expansion α_T and temperature coefficient of adiabatic compressibility β_T in these liquid crystals reveal that they diverge near the transition temperature and attain unusually high values, starting from isotropic and mesophases. The pretransitional effects are prominent on either side of the transition and they are found to be asymmetrical. Figures indicate that anomalous behaviour is exhibited at the isotropic-mesomorphic phase by both parameters α_T and β_T . The anomalies in α_T and β_T are explained by Bendler who suggested that there is a linear coupling (locally) of the order density. Consequently the order fluctuations which becomes large near the transition produce an excess internal pressure and (with enhanced compressibility) result in a more rapid contraction of the fluid. It's assumed that the expansion anomaly is the result of compressibility anomaly. Since Bendler's theory and



Landau de Genne theory are expected to hold good in the high temperature phase, the author has tried to estimate the values of the critical exponent of the isotropic side of the mesomorphic -isotropic transitions. Moreover, the nature of variation indicate that they can be fitted into Bendler's equations.

$$\alpha_T = \alpha_0 + A(T - T^*)^{-r} \quad \beta_T = \beta_0 + B(T - T^*)^{-r'}$$

The results of the thermal expansion coefficient α_T , have been fitted with equation (26) and the results of the temperature coefficient of adiabatic compressibility β_T into equation (30). The experimental data of both parameters have been presented in figures B1 through B5 and B6 through B10 respectively. Here, the author has tried to study the pretansitional effects in three liquid crystals viz PBNP, H6BNP and OBB. The results are presented in Tables B6 through B8. The experimental and theoretical results of α_T are presented in Figures B1, B2 and B5 for PBNP, H6BNP and OBB. The experimental and theoretical results of β_T are presented in Figures B6, B7 and B9 for the same liquid crystals in sequence.

In the Figures the experimental data are depicted as solid lines while the theoretical data are given as points. The values obtained for the critical exponents r , the constants A and α_0 for the thermal expansion coefficient and the critical exponents r' , and the constants B and β_0 for the temperature coefficient of adiabatic compressibility are presented in Table B9. An examination of the Figures indicates that the

agreement between the experimental and theoretical results is good.

The value of $r=1.01$ obtained for OBB for the isotropic phase is in good agreement with the value predicted by de Gennes [46].

The values of 0.71 obtained for PBNP and H6BNP are less than unity but agree reasonably with the value of 0.66 predicted by de Gennes for the nematic phase [61]. The values of r' equal to 2.1 and 1.86 for H6BNP and OBB are in good agreement with the value of 2 since ($r'=r+1$) predicted by de Gennes [46] for the temperature coefficient of adiabatic compressibility in the isotropic phase. The value of 1.74 obtained for PBNP is closer to the value of 1.66 predicted by the same theory for the nematic phase. However the slight differences between the experimental and theoretical values may be due to the temperature control, which varies within the limits of $\pm 0.01^\circ\text{C}$ a limit which may not be sufficiently accurate to study the behaviour very near to the phase transition. The presence of impurities in the samples also can not be ruled out.

It can be seen from the above discussion that the agreement between the theoretical and experimental results is good, thus showing the validity of Bendler's theory in explaining the pre transitional effects in the isotropic phase of liquid crystals. The values of the order parameter S_k obtained at the isotropic mesomorphic phase transition employing Maier Saupe's theory are presented in Table B10. The values of $\Delta V / V_{k,n}$ and $A/T_k V_{k,n}$

are also included. .

The values obtained for S are 0.437, 0.439, 0.441, 0.442 and 0.444 for PBNP, H6BNP, H7BNP, HBB and OBB respectively. These values are in good agreement with the theoretical value of $S=0.4$ predicted by Maier-Saupe theory.

A glance at the temperature variation of the order parameter S (Figure B11 through B15) reveals that the trend of variation of the order parameter with the temperature in the mesomorphic region is uniform for all the liquid crystals studied. However, though these results are necessarily approximate, it enables one to make an estimation of the variation of the vibrational amplitude with temperature from the available ultrasonic data. Starting from the isotropic-mesomorphic phase transition temperature, the order parameter increases uniformly as the temperature decreases. ✓

The Lennard-Jones potential given by equation (10) of section A has been also been analyzed. The results are included in Tables B6 through B10. The results indicate that the Lennard-Jones potential exponent (n) increases with decrease in temperature and attains a minimum at phase transition. Further, in the nematic phase the (n) value increases. This indicates that the Lennard-Jones's potential repulsive term becoming minimum at phase transition, further decrease in temperature, the repulsive term decrease and in the nematic phase it is lower than in the isotropic phase. As can be seen, the Lennard-Jones's

potential exponent (n) values becomes minimum at phase transition, in the isotropic phase it increases with temperature, indicating that the intermolecular forces interplanar and interterminal forces become weak, and in the mesomorphic phase (n) increases with decreasing temperature, indicating that these attractions become stronger hence making it rigid. It can be seen also that as we proceed towards higher members of the homologous series the value of n increases. It also changes with the change of the terminal substituent. If we assume a spherical cage model, the free volume (V_f) is given by equation (12). It can be seen that the decrease in adiabatic compressibility means decrease in free volume, and that is due to the close packing of the molecules.

REFERENCES :

1. Roa, M.R. Ind. J. Phys., 14, 109 (1940)
2. Rao, M.R. J. Chem. Phys., 9, 682 (1941)
3. Lagemann, R.T., J.Chem. Phys., 16, 247 (1948)
McMillan D.R.
and Woosely, M.
4. Wada Y. J. Phys. Soc. Japan, 4, 280 (1949).
5. Schaafs W. Zeits.Naturforsch, 13 A, 396 (1948)
Z. Phys. Chem., 195, 136 (1950)
Ibid, 196, 397, 413 (1951).
6. Schaafs W. Acoustica, 33, 272 (1925).
7. Sodizkiewi E. Archiers of Acustics, 2, 325 (1977).
8. Hildebrand J.M. 'Regular Solutions' Prentice Hall
and Scott R.C. Inc. Eagleswood Cliffs. U.S.A. (1962).
9. Gabrieli I. Novo. Cimen., 2, 326 (1955).
Verdini L.
10. Hoyer W.A. J.Chem. Phys., 24, 803 (1956).
and Nolle A.W.
11. Frenkel. J. Kinetic Theory of Liquids (Dover
Publications Inc. Newyork, 382 (1946).
12. Zavera G.E. Sov. Phys, Cryst., 10, 603 (1966).
Kapustine A.P.
13. Kapustine A.P. Sov. Phys., Cryst., 13, 281 (1968).
and Bykova N.T.
14. Kapustine A.P. Sov. Phys., Cryst. 11, 279 (1966).

15. Semenchenkov V. Sov. Phys., Cryst., 2, 139 (1957).
16. Kapustine A.P. Sov. Phys., Cryst., 16, 559 (1971)
and Martyanova
17. Maier W. and Z. Naturforsch, 13 A, 564 (1958).
and Saupe A.
18. Maier W. and Z. Naturforsch, 14 A, 882 (1959).
and Saupe A.
19. Maier W. and Z. Naturforsch, 15 A, 287 (1958).
and Saupe A.
20. Kartha G.G. & J. Phys. Soc. Jpn., 31, 904 (1971).
Padmini A.R.K.L.
21. Kartha G.G. & Ind. J. Pure abd Appl. Phys., 9, 725
Padmini A.R.K.L. (1971).
22. Fixman M. J. Chem. Phys., 36 1961 (1962).
23. Otia J.R. and Ind. J. Pure and Appl. Phys., 11, 190
Padmini A.R.K.L. (1973).
24. Otia J.R. and Mol. Cryst. Liq. Cryst., 36, 25 (1976).
Padmini A.R.K.L.
25. Kor S.K. and J.Chem. Phys. (U.S.A) . 64, 1333 (1967).
Pandy S.K.
26. Kawamura, Y., Jap.J. App. Phys., 12(10), 1510 (1973).
Maeda Y. and
Iwayanagi S.
27. Landau L.D. and Dokl. Akad. Nauk SSR, 96, 569 (1954).
Khalatnikov I.M.

28. Lagunov A.S., Sov. Phys. Acoust., 22 (1), 76 (1976).
 Nozdrev Y.P.
 and Reztsov
 Yu V.
29. Bhattacharya S., Phys. Rev. A, 22, 2133 (1980).
 Sarma B.K and
 Ketterson J.B.
30. George A.K., Acustica, 47, 149 (1981).
 Vora R.A. and
 Padmini A.R.K.L.
31. George A.K. and Ultrasonics, 271 (1982).
 Padmini A.R.K.L.
32. Bendler J. Mol. Cryst. Liq. Cryst., 38, 19 (1977).
33. Rao N.V.S. and Z. Naturforsch, 37 a, 1262 (1982).
 Pissipati V.K.G.M.
34. Rao N.V.S. and Phase Trans., 3 159 (1983).
 Pissipati V.K.G.M.
35. Rao N.V.S. and Acoustican, 54, 56 (1983).
 Pissipati V.K.G.M.
36. Rao N.V.S., Mol Cryst. Liq. Cryst., 136, 307 (1986).
 Pissipati V.K.G.M.,
 Prasad P.V.
 Datta and
 Alapati P.R.

37. Pisipati V.G.K.M., *Acoustica*, 60, 165 (1986).
 Rao N.V.S.,
 Gauri Shankar Y.
 and Murthy J.S.R.
38. Dhake K.P., *J. Acoust. Soc. Ind Vol. XVII (3 & 4)*
 Bhagwat W.P., 161 Dec. (1989).
 Mahajan H.K.,
 Shaikh I.A.
 and Bhavna T.
39. Dhake K.P., *J. Acoust. Soc. Ind Vol. XVIII (384)*
 Otia J.R., (1990).
 Shaikh I.A.,
 Bhagwat W.P.
 & Neeta Majumdar
40. Dhake K.P. *J. Acoust. Soc. Ind. Vol. XVIII (3 & 4)*
 Mahajan H.K. 36 (1990).
 Patil S.N.,
 Bhavana T.
 and Kekan L.L.
41. George A.K. *Acustica (Germany) 73, 8287 May (1991).*
42. George A.K. *Acoust. Lett. (U.K), 14 8 156 Feb.*
 (1991).
43. Malikarjuna Rao *Ind. J. Pure and App. Phys. (India) 29*
 P and Srinivas 7 503 July (1991).
 Rao A.

44. Malikarjuna Rao Ind.J. Pure and App. Phys.(India) 64
 P and Srinivas A 6 480 Nov (1990)
 Rao A.
45. Landau, L.D. "On the Theory of Phase Transitions,
 Part I and II" Collected Papers of
 L.D. Landau, Edited by D.ter. Haar, P-
 193-216 (1967).
46. de Gennes P.G. Mol. Cryst. Liq. Cryst. 12, 193
 (1971).
47. Cruickshank D.W.J. Acta. Cryst. 9, 1005 (1956).
48. Becka L.D. and Proc. Roy. Soc. A, 273, 455 (1963).
 Cruickshank D.W.J.
49. Chatelain P. Bull. Soc. Franc. Miner Cryst. 78, 262
 (1955).
50. Srinson, J.W. and Phy. Rev. Lett., 25(8), 503 (1970).
 Litser J.D.
51. Yang C.C. Phy. REv. Lett. 28 (15), 955 (1972).
52. de Gennes, P.G. The Physics of Liquid Crystals (Oxford
 University, Press, London, 1975)
 Chapter 2.
53. Chu B., Bak C.S. Phy. Rev. Lett. 28 (17).
 and Lin F.L.
54. Cheung J. and Phy. Rev. Lett. 29(18), 1240 (1972).
 Meyer R.B.

55. Cheung L., Phy. Rev. Lett., 31(6), 349 (1973).
Meyer R.B. and
Crueler H.
56. Delaye M., Phy. Rev. Lett., 31(7), 443 (1973).
Ribotta R and
Durand G.
57. Cladis P.E. Phy. Rev. Lett., 31, 1200 (1973).
58. Djurek D., Phy. Rev. Lett. 33(10), 1126 (1974).
Baturic J. and
Franulovic K.
59. Otia J.R. and J. Pure. Appl. Ultrason. 33, 6(1984).
Padmini A.R.K.L.
60. Kartha C.G. and Mol. Cryst. Liq. Cryst., 243, 29(1975).
Padmini A.R.K.L.
61. de Gennes P.G. Solid St. Commun., 10, 753 (1972).

TABLE A		
Liquid Crystal	Molecular Weight	Transition Temperature T°c
PBNP	333	(62)
H6BNP	347	(65)
H7BNP	361	(56)
HBB	344	55-62
OBB	358	60-70

Values given in brackets indicate monotropy

PBNP					
TABLE A1					
Temperature T °C	Ultrasonic Velocity V m/sec.	Density S g/cm ³	Adiabatic compressibility K _{ad} x 10 ¹² cm ² /dyne	Molar Sound velocity (R)	Wada constant (B)
54	1405	1.1741	43.15	3176.61	165.642
55	1401	1.1730	43.43	3176.57	165.644
56	1398	1.1719	43.66	3177.28	165.670
57	1396	1.1707	43.83	3179.02	165.670
58	1392	1.1695	44.12	3179.24	165.750
59	1388	1.1684	44.43	3179.18	165.760
60	1385	1.1673	44.66	3179.88	165.750
61	1380	1.1660	45.03	3179.59	165.790
61.5	1373	1.1652	45.54	3176.39	165.779
61.8	1368	1.1646	45.88	3173.61	165.626
62	1365	1.1645	46.08	3172.11	165.507
62.2	1385	1.1638	44.81	3190.27	165.447
62.5	1392	1.1633	44.37	3196.46	166.252
63	1395	1.1626	44.20	3200.40	166.529
64	1392	1.1615	44.43	3201.14	166.706
65	1389	1.1602	44.67	3202.40	166.741
66	1385	1.1591	44.98	3202.38	166.799
67	1382	1.1580	45.21	3203.10	166.792
68	1380	1.1569	45.39	3204.60	166.829
69	1379	1.1558	45.50	3206.88	166.893

H6BNP					
TABLE A2					
Temperature T °C	Ultrasonic Velocity V m/sec.	Density S g/cm ³	Adiabatic compressibility K _{ad} x 10 ¹² cm ² /dyne	Molar Sound velocity (R)	Wada constant (B)
58	1383	1.1480	45.54	3367.66	175.175
59	1380	1.1469	45.78	3368.45	175.212
60	1377	1.1457	46.03	3369.53	175.259
61	1374	1.1445	46.28	3370.61	175.307
62	1370	1.1433	46.60	3370.87	175.862
63	1366	1.1421	46.92	3371.13	175.331
64	1364	1.1410	47.18	3372.73	175.282
64.5	1361	1.1404	47.33	3372.03	175.374
64.8	1358	1.1400	47.58	3370.73	175.309
65	1354	1.1395	47.87	3370.37	175.229
65.2	1351	1.1390	48.10	3367.88	175.185
65.5	1370	1.1385	46.80	3385.08	175.950
66	1375	1.1380	46.48	3390.69	176.200
67	1373	1.1370	46.66	3392.02	176.257
68	1371	1.1358	46.84	3393.96	176.346
69	1369	1.1345	47.03	3396.19	176.446
70	1366	1.1334	47.28	3397.00	176.484
71	1362	1.1323	47.61	3396.98	176.480
72	1359	1.1311	47.87	3398.09	176.530
73	1356	1.1301	48.12	3398.59	176.555

H7BNP					
TABLE A3					
Temperature T °C	Ultrasonic Velocity V m/sec.	Density S g/cm ³	Adiabatic compressibility K _{ad} × 10 ¹² cm ² /dyne	Molar Sound velocity (R)	Wada constant (B)
48	1368	1.1442	46.7	3502.41	182.1928
49	1366	1.1430	46.88	3504.38	182.2840
50	1363	1.1416	47.15	3506.1	182.3578
51	1360	1.1403	47.41	3507.52	182.4223
52	1358	1.1390	47.6	3509.8	182.5262
53	1356	1.1377	47.8	3512.09	182.6253
54	1353	1.1364	48.06	3517.84	182.6926
55.5	1350	1.1350	48.34	3515.24	182.7662
55.8	1348	1.1343	48.51	3515.67	182.7873
56	1345	1.1341	48.75	3514.3	182.6907
56.2	1341	1.1334	49.06	3512.36	182.6381
56.5	1356	1.1326	48	3524.9	183.3383
57	1359	1.1324	47.81	3531.13	183.4746
58	1360	1.1312	47.79	3535.74	183.6803
59	1358	1.1305	47.96	3536.19	183.7007
60	1356	1.1294	48.15	3537.9	183.7758
61	1353	1.1283	48.41	3538.73	183.8135
62	1350	1.1271	48.68	3539.8	183.8631
63	1357	1.1260	48.94	3540.71	183.9027
64	1345				

HBB					
TABLE A4					
Temperature T °C	Ultrasonic Velocity V m/sec.	Density S g/cm ³	Adiabatic compressibility K _{ad} x 10 ¹² cm ² /dyne	Molar Sound velocity (R)	Wada constant (B)
53	1382	1.0355	50.5631	3700.3633	189.6721
54	1379	1.0344	50.8374	3701.6160	189.7271
55	1376	1.0332	51.1186	3703.2261	189.7979
56	1373	1.0321	51.3969	3704.4764	189.8528
57	1370	1.0310	51.6773	3705.7258	189.9077
58	1366	1.0299	52.0360	3706.0700	189.9228
59	1363	1.0285	52.3364	3708.3969	190.0250
60	1359	1.0273	52.7116	3709.0992	190.0529
61	1351	1.0257	53.4157	3707.5744	189.9889
61.4	1343	1.0246	54.1120	3697.7181	189.8413
62	1329	1.0234	55.3229	3695.6762	189.4640
62.3	1351	1.0221	53.6038	3720.6331	190.5624
63	1353	1.0217	53.4664	3723.9254	190.7069
64	1354	1.0209	53.4293	3727.7614	190.8752
65	1353	1.0201	53.5503	3729.7663	190.9032
66	1351	1.0193	53.7511	3730.8536	191.0109
67	1349	1.0185	53.9530	3731.9407	191.0586
68	1347	1.0176	54.1611	3733.3945	191.1225
69	1345	1.0168	54.3651	3734.4817	191.1701
70	1343	1.0160	54.5700	3735.5688	191.2179

OBB					
TABLE A5					
Temperature T °C	Ultrasonic Velocity V m/sec.	Density S g/cm ³	Adiabatic compressibility K _{ad} x 10 ¹² cm ² /dyne	Molar Sound velocity (R)	Wada constant (B)
60	1369	1.0127	52.6881	3925.2743	200.6519
61	1365	1.0117	53.0497	3925.3237	200.6504
62	1361	1.0108	53.4095	3924.9773	200.6389
63	1357	1.0099	53.7727	3924.6229	200.6234
64	1354	1.0090	54.0594	3925.2266	200.6498
65	1351	1.0081	54.3483	3925.8274	200.6761
66	1347	1.0072	54.7204	3925.4536	200.6598
67	1343	1.0063	55.0961	3925.0714	200.643
68	1340	1.0055	55.3871	3925.2672	200.6516
68.8	1336	1.0046	55.7691	3924.8706	200.6342
69.1	1333	1.0042	56.0428	3923.4928	200.5738
69.5	1330	1.0038	56.3183	3922.1093	200.5132
70	1317	1.0020	57.3388	3916.3113	200.3588
70.5	1322	1.0008	57.1728	3925.9633	200.6821
70.7	1326	1.0004	56.8512	3931.4902	200.9242
71	1330	0.9995	56.0606	3938.9828	201.2524
72	1332	1.9987	56.4360	3944.1132	201.4771
73	1330	0.9979	56.6513	3945.2985	201.529
74	1326	0.9970	57.0450	3944.8975	201.5114
75	1322	0.9962	57.4368	3944.0916	201.4761
76	1319	0.9954	57.7448	3944.2731	201.4841
77	1315	0.9945	58.1492	3943.8479	201.4654
78	1311	0.9936	58.5576	3943.4136	201.4464
79	1307	0.9928	58.9640	3942.5732	201.4096

PBNP					
TABLEB1					
Temperature T °C	α_T	B _T	Molar Volume	Available Volume V	n
54	10.220	7.9481	283.6215	34.5664	36.2307
55	10.351	8.2155	283.8875	35.3085	35.2412
56	10.524	8.7528	284.1539	35.8744	34.5248
57	10.591	9.7656	284.4452	36.3668	34.0588
58	10.688	10.6336	284.7370	37.0158	33.1539
59	11.126	11.9357	285.0015	37.7632	32.2824
60	11.993	15.4079	285.2737	38.3337	31.6511
61	12.864	22.7864	285.5918	39.2689	30.6363
61.5	12.015	23.4374	285.7878	40.5461	29.1472
61.8	42.933	21.7013	285.9351	41.4606	28.3793
62			285.9596	42.0003	27.8485
62.2	30.070	137.8038	286.1316	38.4489	31.6512
62.5	22.352	74.2187	286.2792	37.2163	33.1538
63	16.342	40.7986	286.4270	36.6985	33.8292
64	12.914	17.9036	286.6982	37.2355	33.1976
65	12.354	10.1996	287.0195	37.8507	32.4976
66	11.646	5.9678	287.2919	38.6048	31.6512
67	11.226	3.7760	287.5648	39.1807	31.0367
68	10.948	2.9947	287.8382	39.5778	30.8363
69	10.753	1.7981	288.1120	39.7955	30.4389

H6BNP		TABLEB2			
Temperature T °C	α_T	B_T	Molar Volume	Available Volume V	n
58	10.577	6.9533	302.2648	40.9947	31.2396
59	10.753	7.2766	302.5547	41.6013	30.6363
60	10.823	7.6874	302.8716	42.2127	30.0494
61	10.921	8.3037	303.1897	42.8255	29.4779
62	11.079	8.8433	303.5074	43.6299	28.7432
63	11.382	9.9227	303.8263	44.4346	28.0256
64	11.315	14.4140	304.1192	44.8576	27.6779
64.5	15.783	22.5611	304.2792	45.4517	27.1664
64.8	21.929	30.2903	304.3860	46.0384	26.6694
65			304.5195	46.8199	26.0244
65.2	2121.195	24.0233	304.6532	47.4117	28.5542
65.5	17.566	44.7044	304.7870	43.8131	28.7392
66	13.181	29.0369	304.9209	42.8795	29.6667
67	10.993	12.6383	305.1891	43.2987	29.2908
68	10.858	7.1722	305.5115	43.7263	28.9214
69	11.000	4.3868	305.8616	44.1588	28.5584
70	10.746	2.4650	306.1585	44.7757	28.0256
71	10.597	0.9052	306.4559	45.5853	27.3361
72	10.609	0.0000	306.7810	46.2089	26.834
73	10.397	0.6528	307.0525	46.8255	26.3443

H7BNP TABLE B3					
Temperature T °C	α_T	B_T	Molar Volume	Available Volume V	n
48	11.798	6.0130	315.5043	45.7481	28.3973
49	11.998	6.3479	315.8355	46.1909	28.0257
50	11.971	6.4886	316.2228	46.8405	27.5003
51	11.210	6.7264	316.5834	47.4875	27
52	12.291	7.4398	316.9447	47.9379	26.6694
53	12.598	8.5609	317.3068	48.3893	26.3443
54	13.199	10.1916	317.6698	49.0403	25.8664
55	14.096	14.6759	318.0617	49.6971	25.4
55.5	15.866	22.4215	318.2580	50.1256	25.0953
55.8	30.861	31.5939	318.3141	50.7313	24.6471
56			318.5107	51.5589	24.0657
56.2	3.532	108.0309	318.7357	48.6072	26.3443
56.5	17.661	50.9580	318.7920	48.0180	26.8341
57	19.448	25.8866	319.1301	47.8695	27
58	12.826	11.2107	319.3280	48.2984	26.6694
59	11.805	6.1829	319.6387	48.7449	26.3443
60	11.300	3.3122	319.9503	49.3923	25.8664
61	11.179	1.5491	320.2910	50.0455	25.3999
62	10.953	0.4076	320.6039	50.5955	25.0197

HBB					
TABLE B4					
Temperature T °C	α_T	B_T	Available Volume V_L	Molar Volume	n
52	11.7806	8.8764	44.8436	332.1746	31.4444
53	12.9835	9.5596	45.2631	332.2066	31.0367
54	13.2927	10.1348	45.9348	332.5599	30.4389
55	13.5501	10.8565	46.6125	332.9462	29.8571
56	14.0490	11.8275	47.2871	333.3010	29.2907
57	14.7430	13.1794	47.9631	333.6566	28.7392
58	15.7782	14.8533	48.8494	334.0130	28.0256
59	16.5289	17.9944	49.5430	334.4677	27.5064
60	18.9818	23.6005	50.4380	334.8584	26.8341
61	22.4237	34.474	52.1936	335.3807	25.5542
61.4	19.5198	36.4748	53.9284	335.7408	24.3541
62			56.9328	336.1345	22.4243
62.3	42.3964	103.5797	52.3775	336.5620	24.5542
63	16.6359	33.5575	51.9771	336.6937	25.8664
64	12.2441	17.1141	51.8072	336.9576	26.0244
65	10.7833	10.6863	52.0586	337.2218	25.8664
66	10.0559	7.1028	52.5213	337.4865	25.5542
67	9.6220	4.9524	52.9848	337.7516	25.2470
68	9.4995	3.50006	53.4542	338.0503	24.9497
69	9.2728	2.4733	53.9192	338.3163	24.6470
70	9.1043	1.7011	54.3848	338.5827	24.3541

HBB TABLE B5					
Temperature T °C	α_T	B_T	Molar Volume	Available Volume V	n
60	10.5658	8.1109	353.5104	51.0381	28.5584
61	10.6531	8.3114	353.8598	51.9732	27.8510
62	10.8825	8.556	354.1749	52.9049	27.1673
63	11.1751	8.8848	354.4905	53.8382	26.5062
64	11.5626	9.5322	354.8067	54.5515	26.0244
65	12.1020	10.4309	355.1235	55.2661	25.5542
66	12.9071	11.4164	355.4408	56.2041	24.9446
67	14.2436	13.0377	355.7687	57.1453	24.3541
68	17.4043	17.019	356.0418	57.8568	23.9231
68.8	21.5675	22.8132	356.3607	58.7995	23.3636
69.1	24.3422	25.1139	356.5027	59.4914	22.9550
69.5	35.8637	35.5954	356.6447	60.1838	22.5556
70			357.2854	63.1949	20.9222
70.5	23.9808	15.79014	357.7138	62.1528	21.5324
70.7	22.8480	12.1483	357.8569	61.2830	22.0365
71	25.0125	13.5719	358.1791	60.4427	22.5556
72	16.5215	7.8775	358.4660	60.6431	22.8209
73	13.6954	3.9967	358.7534	60.5396	22.5556
74	12.5376	1.2809	359.0772	61.3207	22.1344
75	11.6442	0.34183	359.3656	62.4398	21.5324
76	11.0508	0.118	359.6544	62.9887	21.259
77	10.7735	0.2019	359.9799	63.9433	20.778
78	10.5676	0.2567	360.306	65.0802	20.218
79	10.2964	0.3149	360.5062	66.0342	19.7645

PBNP				
TABLE B6				
Reduced Temperature T/T _c	Velocity V m/sec	Density S gm/cm ³	θ _{rms}	Order Parameter S
1 0000	1365	1.1741	39°32'	0.4370
0.9994	1368	1.1730	39°20'	0.4416
0.9985	1373	1.1719	39°	0.4489
0.9970	1380	1.1707	38°32'	0.4590
0.9940	1385	1.1695	38° 7'	0.4682
0.9910	1388	1.1684	37°48'	0.4748
0.9881	1392	1.1673	37°27'	0.4825
0 9851	1396	1 1660	37° 6'	0.4901
0.9821	1398	1.1652	36°52'	0.4954
0 9791	1401	1.1646	36°34'	0 5018
0.9761	1405	1.1645	36°14'	0 5092

H6BNP TABLE B7				
Reduced Temperatrure T/Tc	Velocity V m/sec	Density S gm/cm ³	θrms	Order Parameter S
1.0000	1354	1.1395	39°87'	0.4390
0.9994	1358	1.1400	39°11'	0.4448
0.9985	1361	1 1404	38°58'	0.4495
0.9970	1364	1.1410	38°44'	0 4548
0.9941	1366	1 1421	38°29'	0 4603
0.9911	1370	1.1433	38° 7'	0.4682
0.9882	1374	1.1455	37°45'	0.4760
0.9852	1377	1.1457	37°27'	0.4826
0.9822	1380	1.1469	37° 9'	0.4891
0 9793	1383	1.1480	36°51'	0.4956

H7BNP TABLE B8				
Reduced Temperature T/T _c	Velocity V m/sec	Density S gm/cm ³	θ _{rms}	Order Parameter S
1.0000	1345	1.1442	39°22'	0.4410
0.9994	1348	1.1430	39°10'	0.4454
0.9985	1350	1.1416	39°	0.4491
0.9939	1353	1.1403	38°37'	0.4574
0.9909	1356	1.1390	38°18'	0.4643
0.9878	1358	1.1377	38° 2'	0.4700
0.9848	1360	1.1364	37°46'	0.4755
0.9818	1363	1.1350	37°25'	0.4822
0.9787	1366	1.1343	37° 9'	0.4890
0.9757	1368	1.1341	36°54'	0.4944

HBB				
TABLE B9				
Reduced Temperature T/T _c	Velocity V m/sec	Density S gm/cm ³	θ _{rms}	Order Parameter S
1.0000	1329	1.0234	39°16'	0.4430
0.9982	1343	1.0246	38°21'	0.4630
0.9970	1351	1.0257	37°50'	0.4744
0.9940	1359	1.0273	37°14'	0.4873
0.9910	1363	1.0285	36°52'	0.4973
0.9881	1366	1.0299	36°34'	0.5017
0.9851	1370	1.0310	36°13'	0.5093
0.9821	1373	1.0321	35°56'	0.5156
0.9791	1376	1.0332	35°38'	0.5219
0.9761	1379	1.0344	35°21'	0.5282
0.9731	1382	1.0355	35° 4'	0.5344
0.9701	1384	1.0366	34°51'	0.5389

OBB				
TABLE B10				
Reduced Temperature T/T _c	Velocity V m/sec	Density S gm/cm ³	θ _{rms}	Order Parameter S
1.0000	1317	1.0020	39°14'	0.4440
0.9985	1330	1.0038	38°22'	0.4628
0.9974	1333	1.0042	38° 8'	0.4677
0.9965	1336	1.0046	37°55'	0.4724
0.9942	1340	1.0055	37°35'	0.4797
0.9913	1343	1.0063	37°17'	0.4861
0.9883	1347	1.0072	36°56'	0.4958
0.9854	1351	1.0081	36°35'	0.5018
0.9825	1354	1.0090	36°18'	0.5077
0.9800	1357	1.0099	36°	0.5140
0.9767	1361	1.0108	35°40'	0.5213
0.9738	1365	1.0117	35°20'	0.5285
0.9708	1369	1.0127	34°59'	0.5358

TABLE B11			
Liquid Crystal	$\Delta V_k/V_{k,n}$	$A/KT_k V_{k,n}^2$	S_k
PBNP	$1.716 \cdot 10^{-3}$	4.535	0.437
H6BNP	$1.843 \cdot 10^{-3}$	4.536	0.439
H7BNP	$2.028 \cdot 10^{-3}$	4.538	0.441
HBB	$3.127 \cdot 10^{-3}$	4.541	0.442
OBB	$3.393 \cdot 10^{-3}$	4.543	0.444

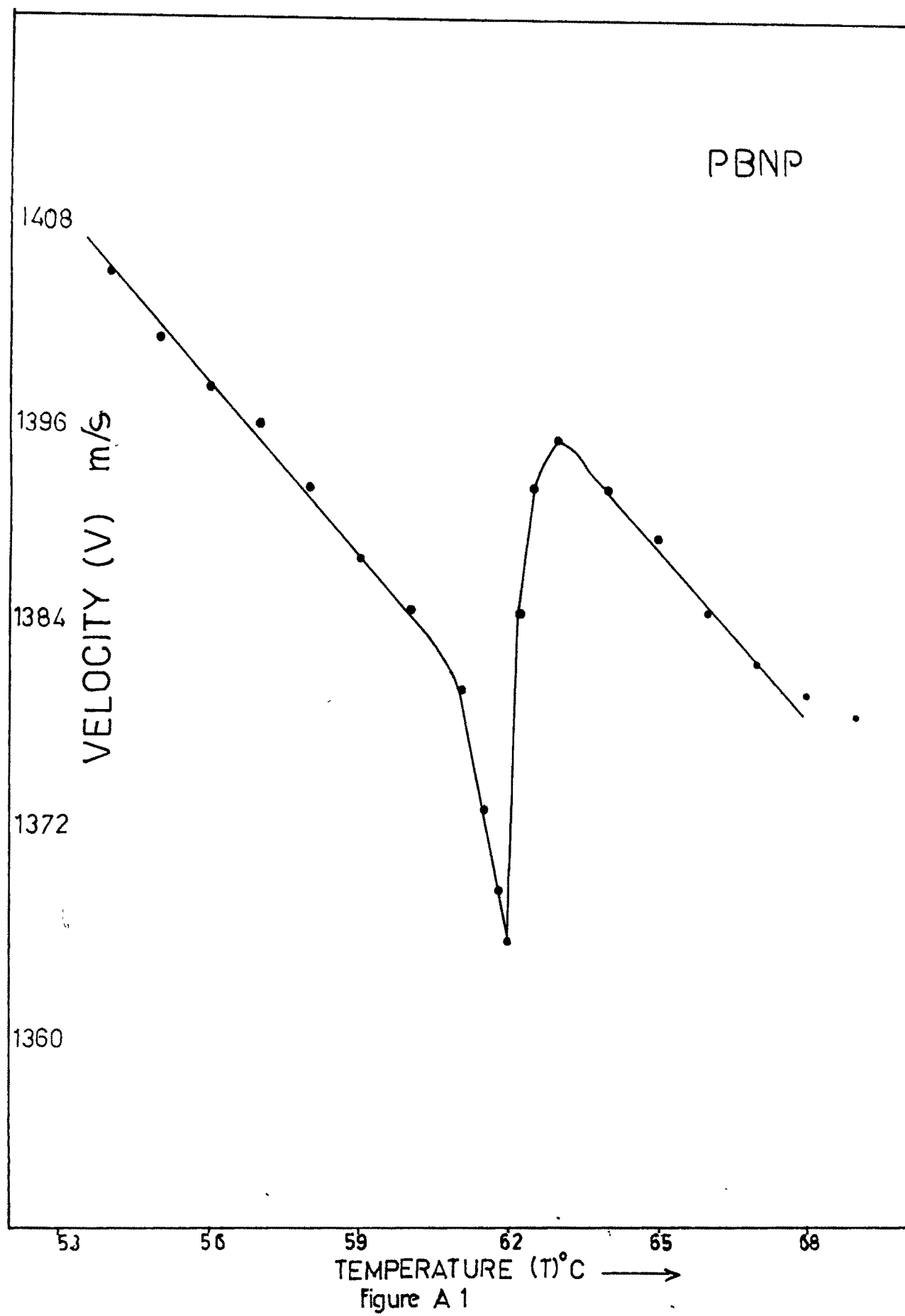
9

PBNP				
TABLE B12				
Temperature T °C	Thermal Expansion coefficient α_T		Thermal Coefficient of ad. comp B_T	
	Experimenta	Theoritical	Experiment	Theoritical
62.2	30.07	30.24	137.80	102.02
62.5	22.35	19.82	74.22	54.60
63	16.34	15.40	40.90	29.58
64	12.91	12.70	17.40	19.58
65	12.35	11.64	10.20	10.19
66	11.65	11.05	5.97	6.58
67	11.23	10.67	3.78	3.76
68	10.95	10.40	2.99	3.19
69	10.75	10.20	1.80	2.68

H6BNP TABLE B13				
Temperature T °C	Thermal Expansion coefficient α_T		Thermal Coefficient of ad. comp B_T	
	Experimenta	Theoretical	Experiment	Theoretical
62.2	21.19	22.45	24.02	54.50
65.5	17.57	15.82	44.70	38.60
66	13.18	13.01	29.04	29.33
67	10.99	11.29	12.64	10.33
68	10.86	10.62	7.17	7.00
69	11.02	10.24	4.39	5.86
70	10.75	10.10	2.47	5.35
71	10.60	9.83	0.91	5.08
72	10.61	9.70	0.00	4.92
73	10.40	9.60	0.65	4.82

OBB TABLE B14			
Thermal Expansion coefficient α_T		Thermal Coefficient of ad. comp β_T	
Experimenta	Theoritical	Experimenta	Theoritical
23.98	23.91	15.70	12.71
22.85	22.27	12.19	10.07
20.01	20.43	13.58	9.08
16.52	16.95	7.87	7.45
13.70	15.21	3.99	3.51
12.54	14.16	1.28	2.06
11.64	13.46	0.34	1.36
11.05	12.96	0.12	0.97
10.77	12.59	0.20	0.73
10.57	12.30	0.26	0.57
10.3	11.07	0.31	0.4

TABLE B15						
Liquid Crystal	α_0	A	r	B ₀	B	r'
PBNP	8.45×10^{-4}	6.95×10^{-4}	0.71	0.012	0.62	1.74
H6BNP	8.59×10^{-4}	4.42×10^{-4}	0.71	0.03	0.25	2.1
OBB	9.98×10^{-4}	21.90×10^{-4}	1.01	0.01	0.27	1.86



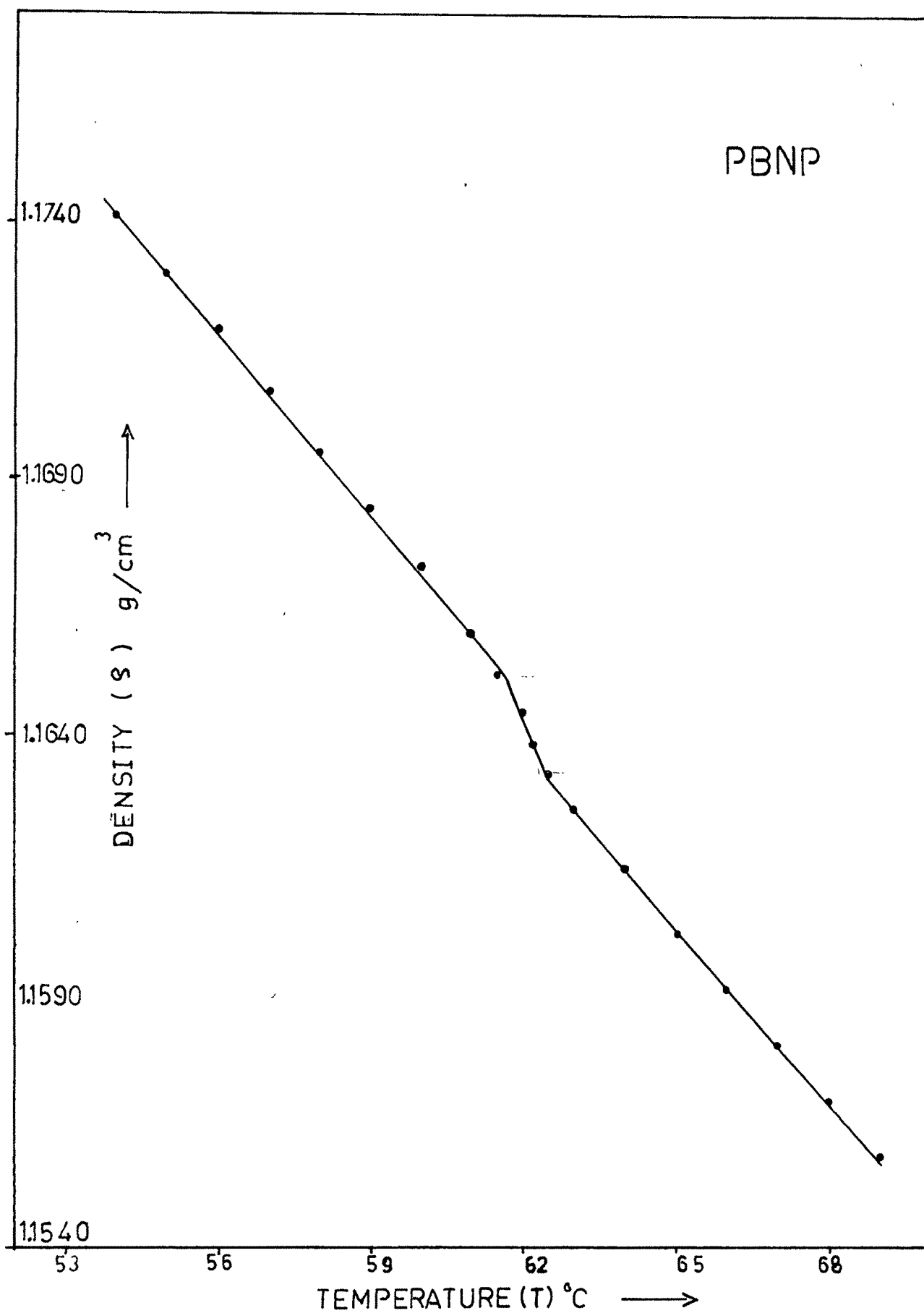


Figure A 2

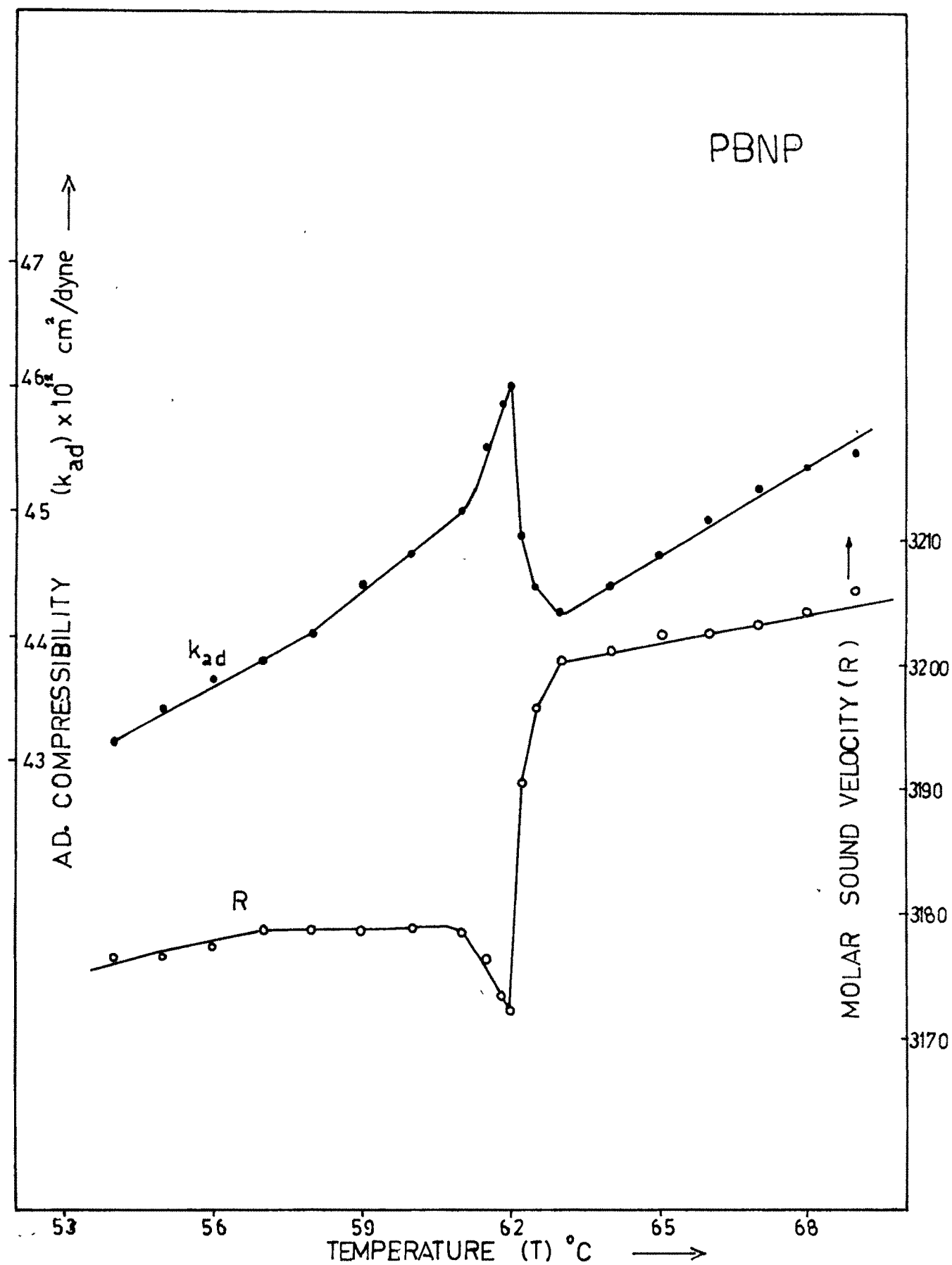


Figure A3

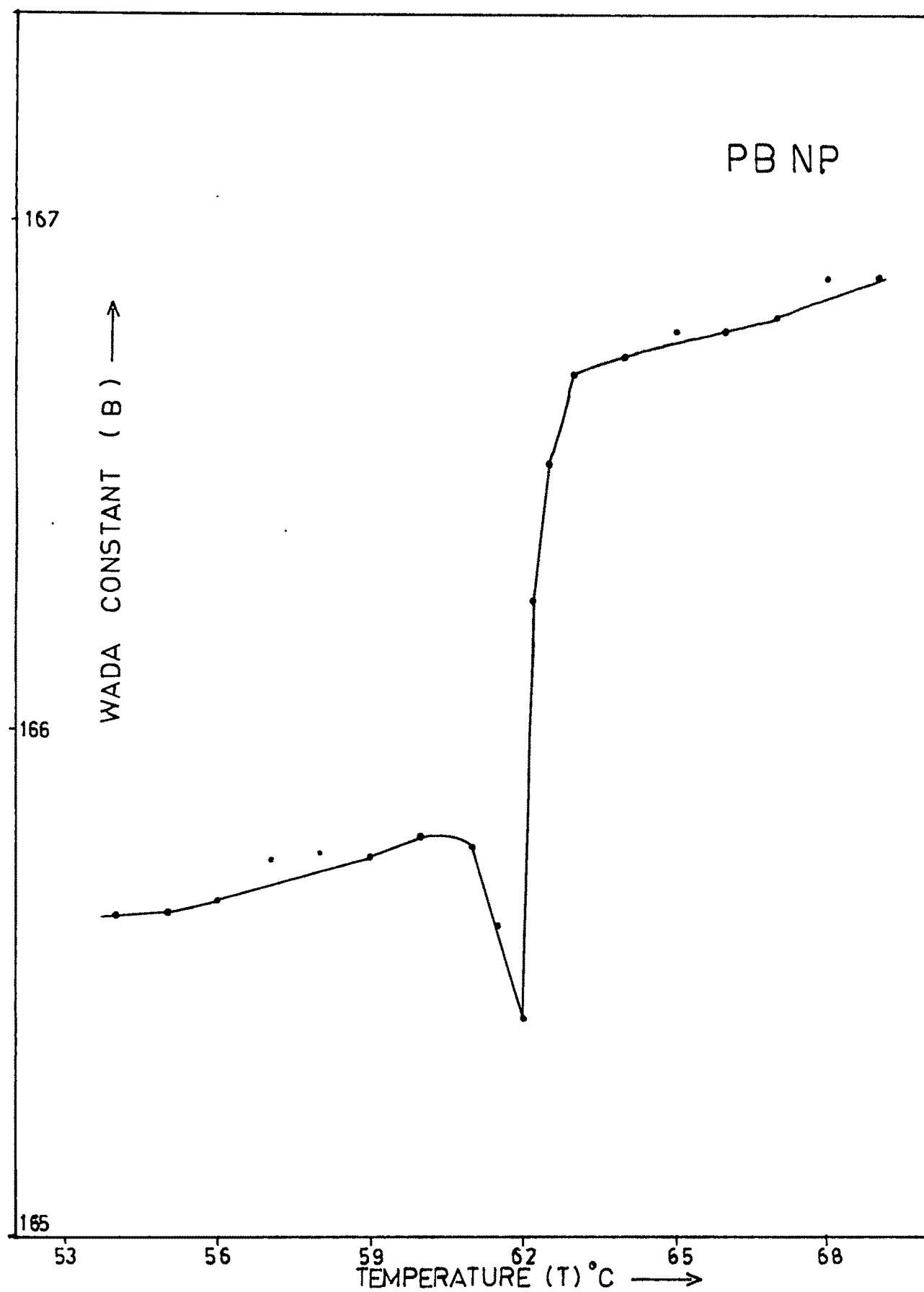


Figure A 4

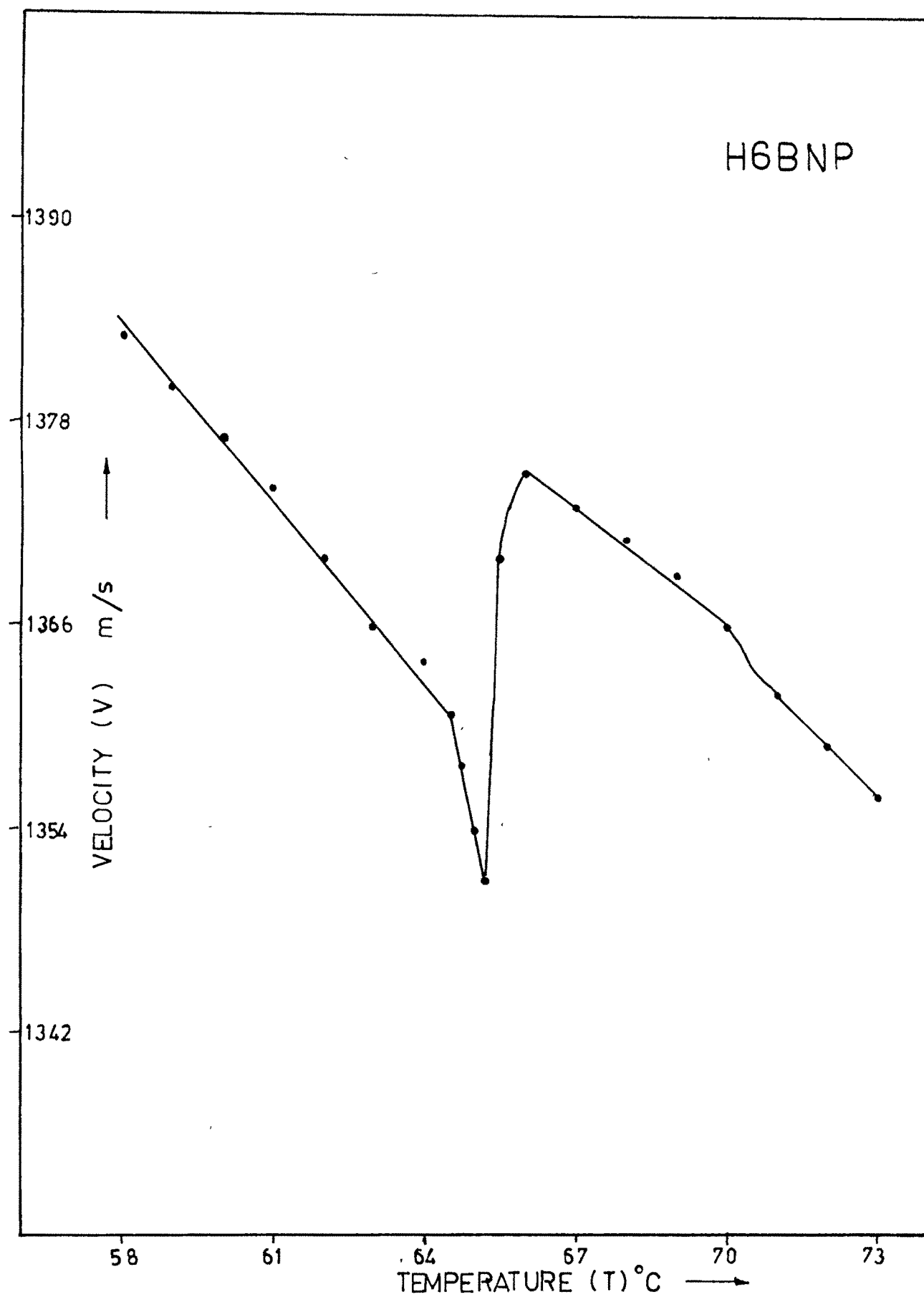


Figure A 5

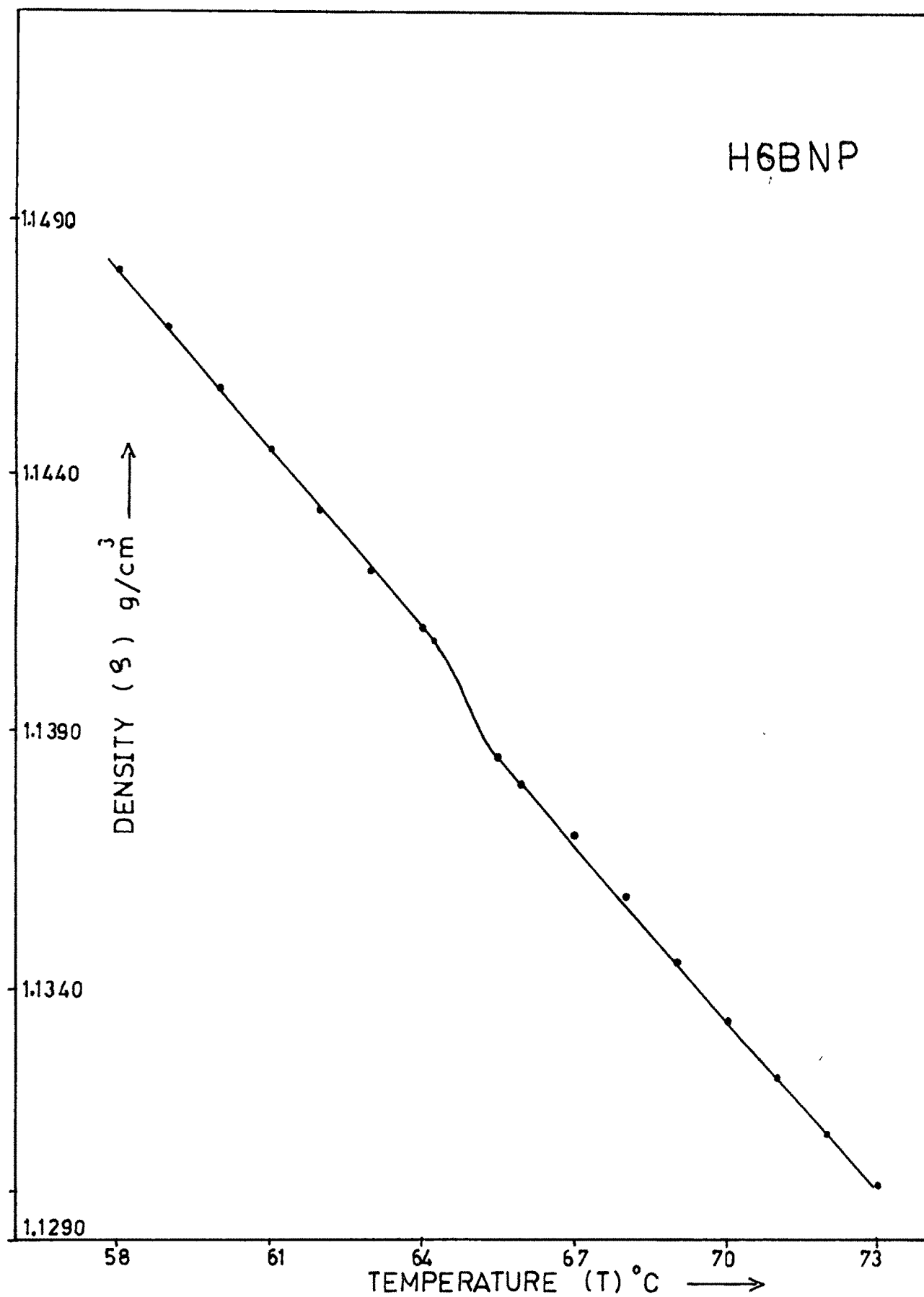


Figure A 6

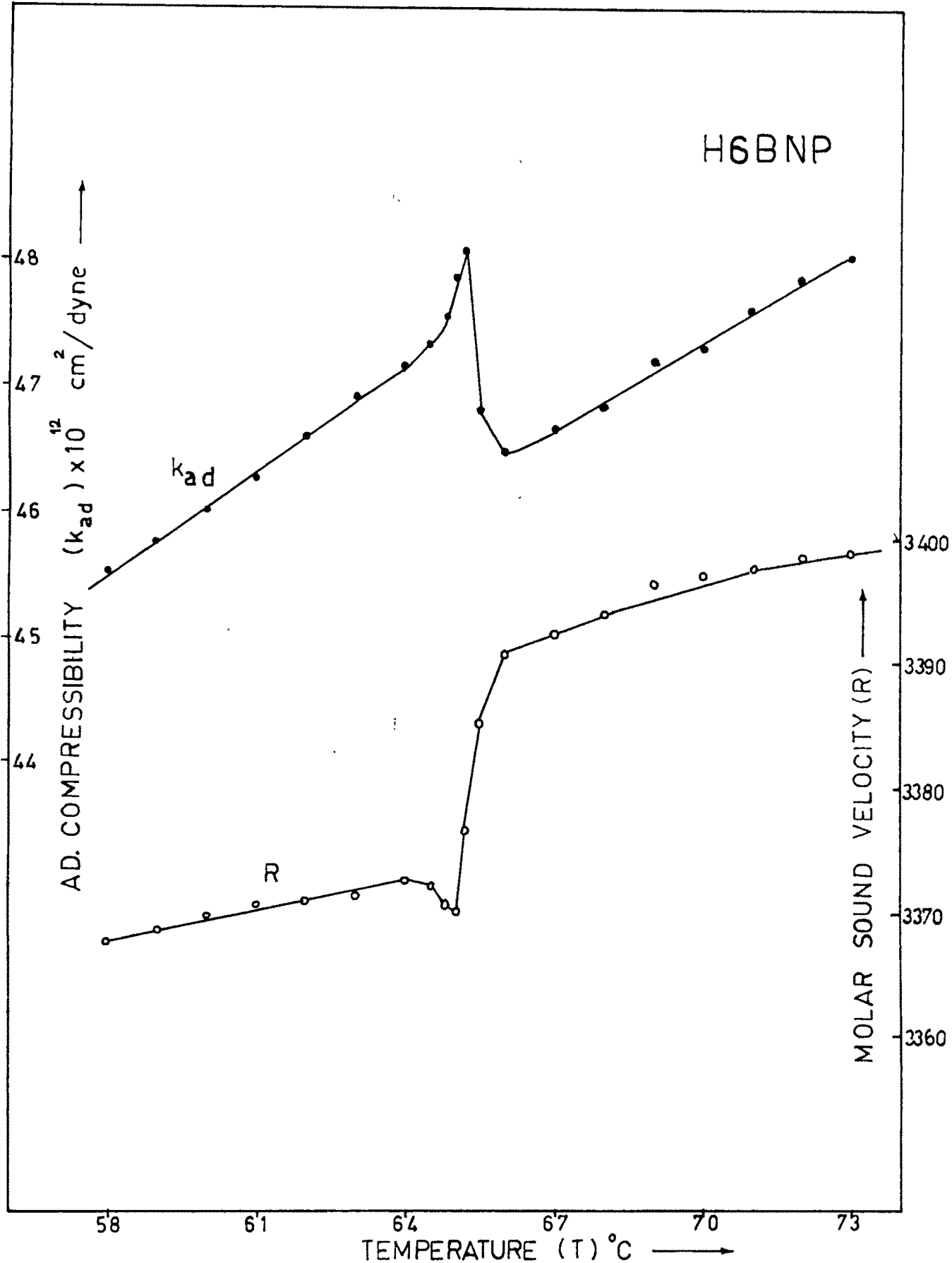


Figure A 7

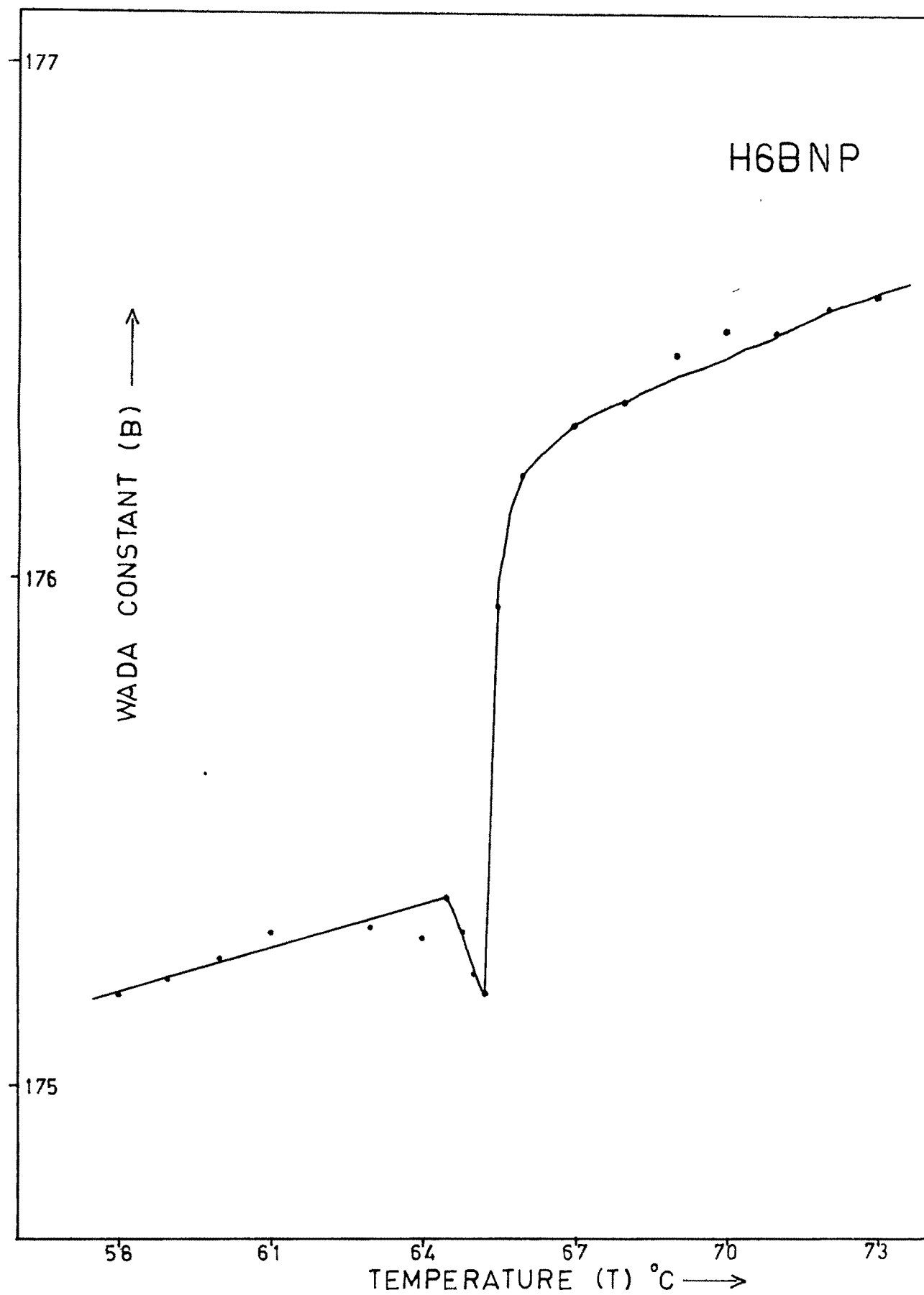
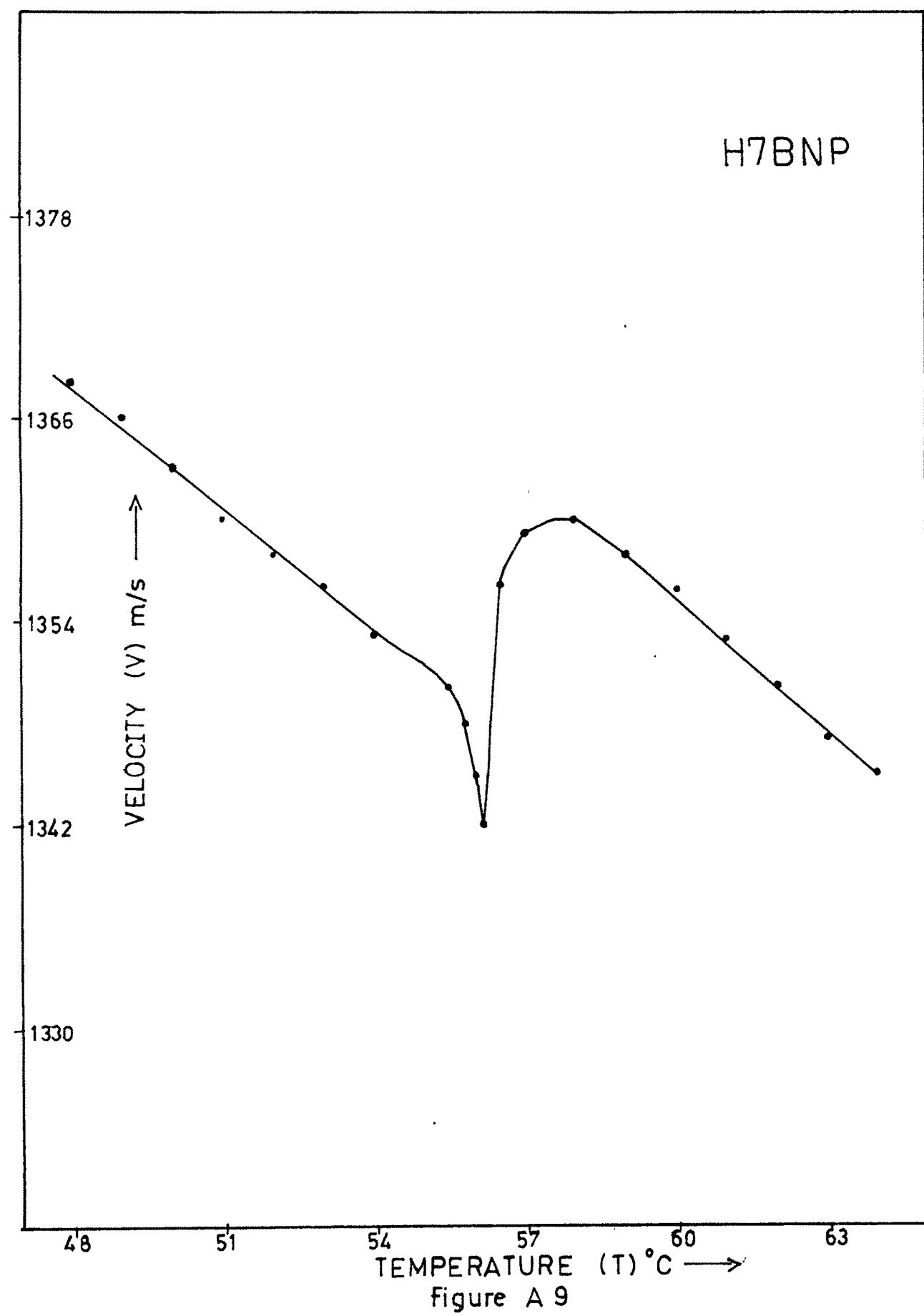


Figure A 8



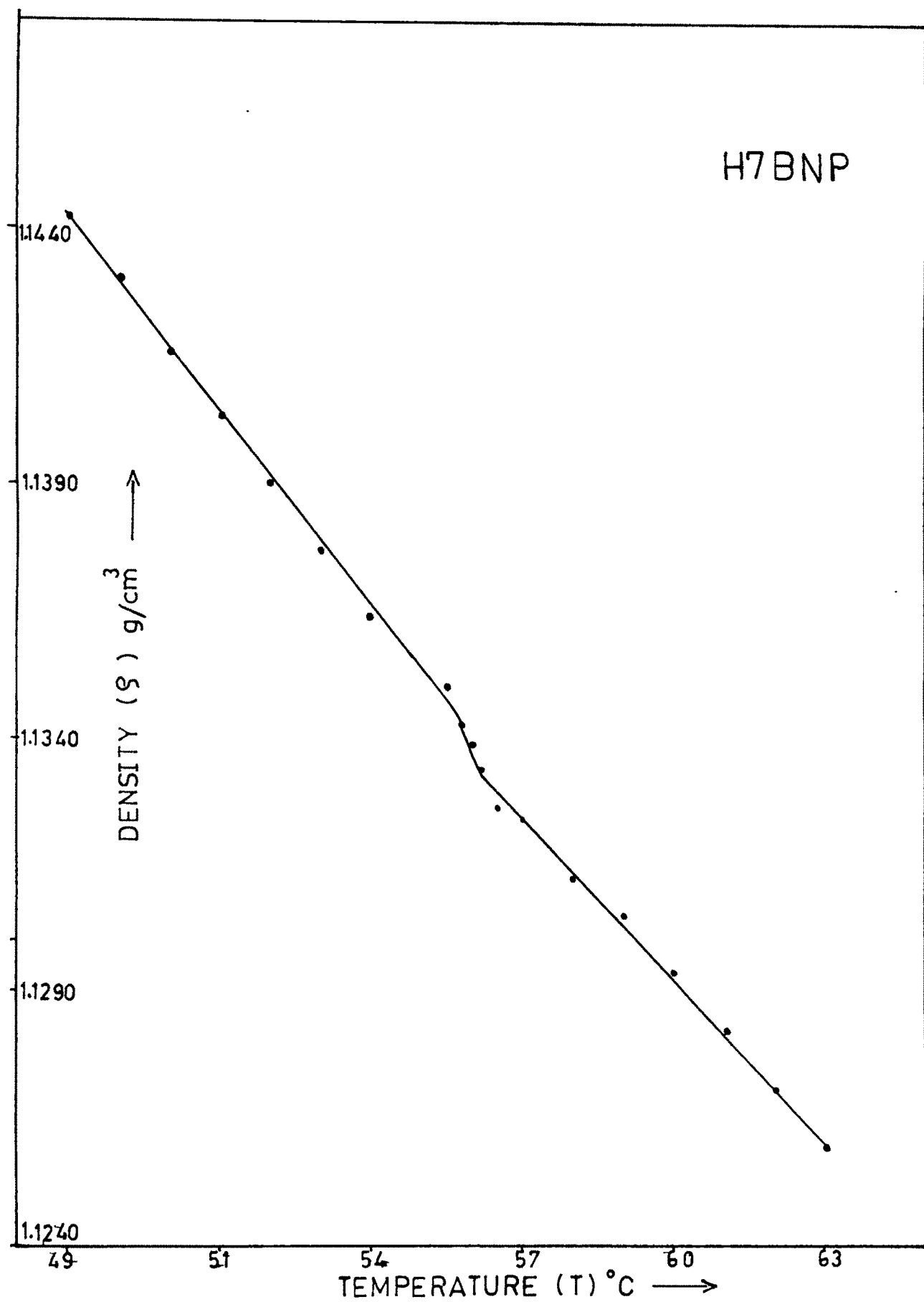


Figure A 10

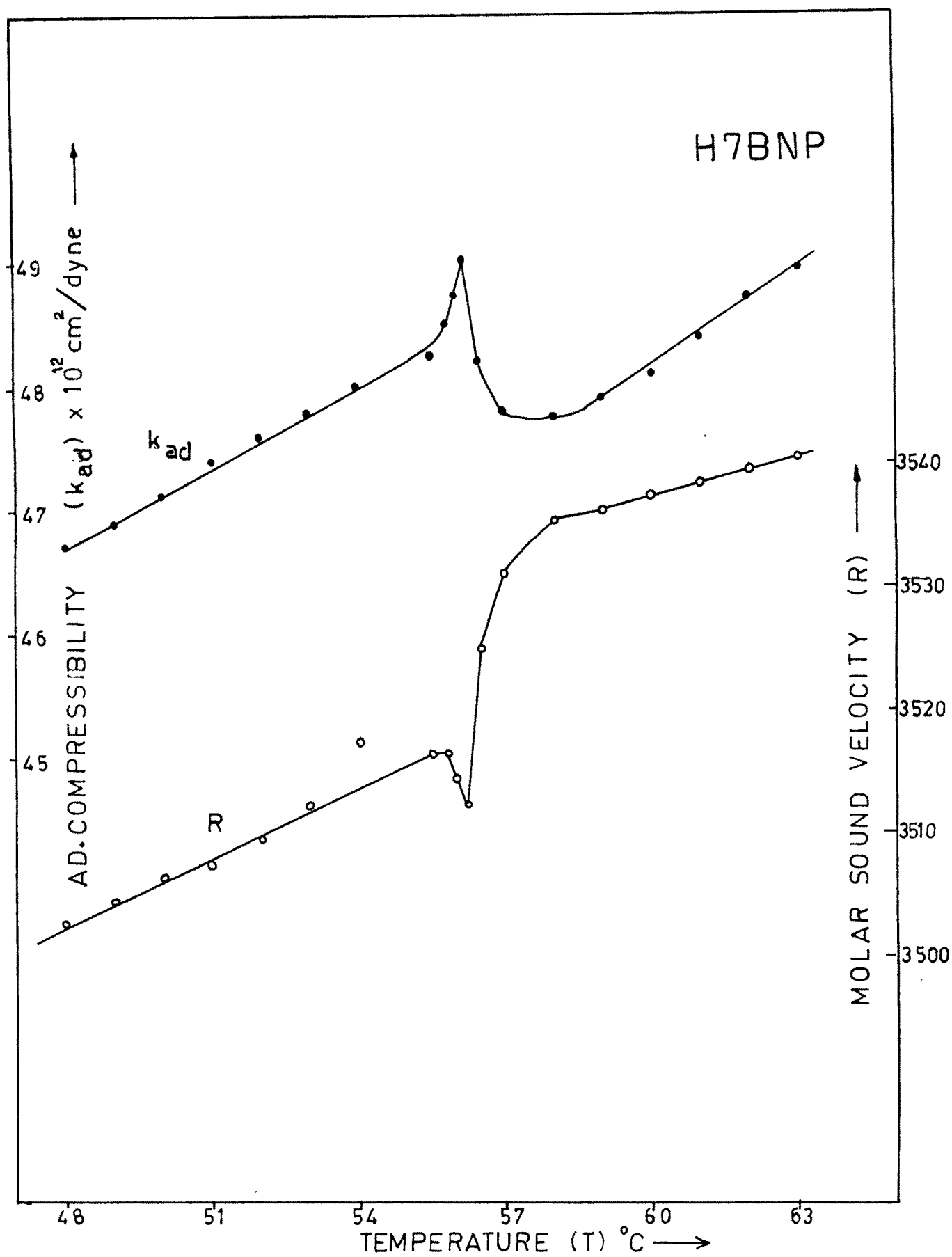


Figure A 11

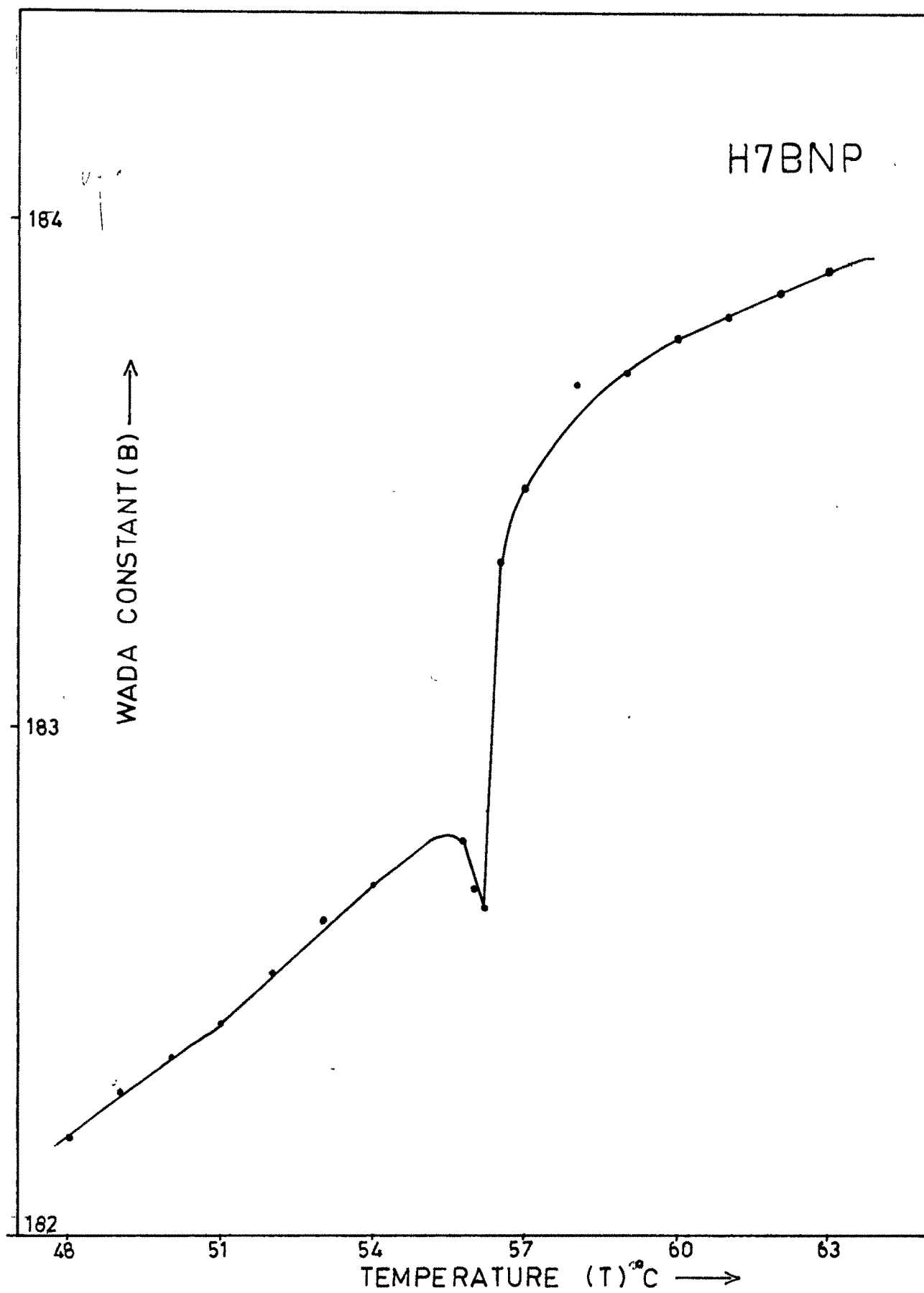


Figure A 12

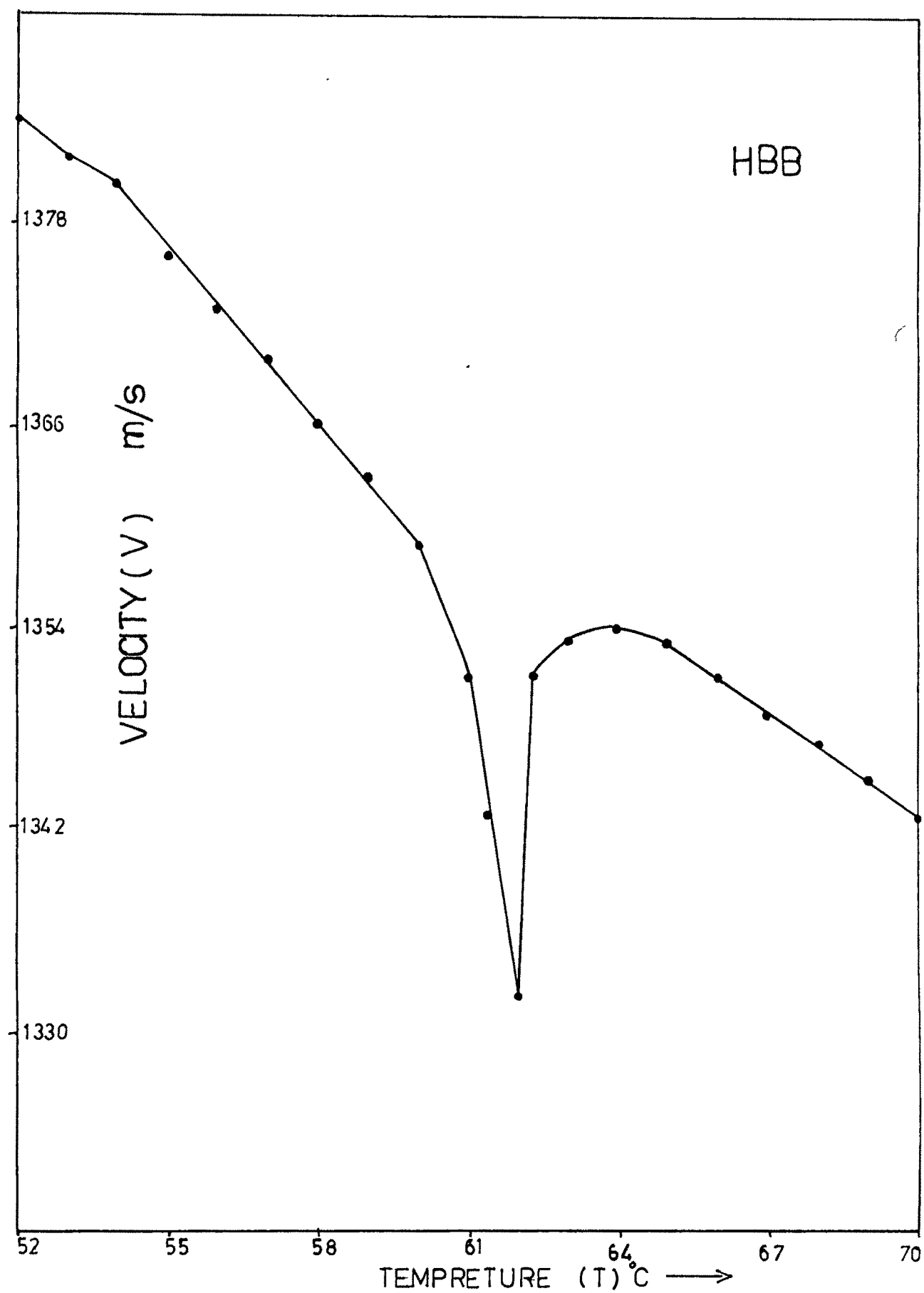


Figure A13

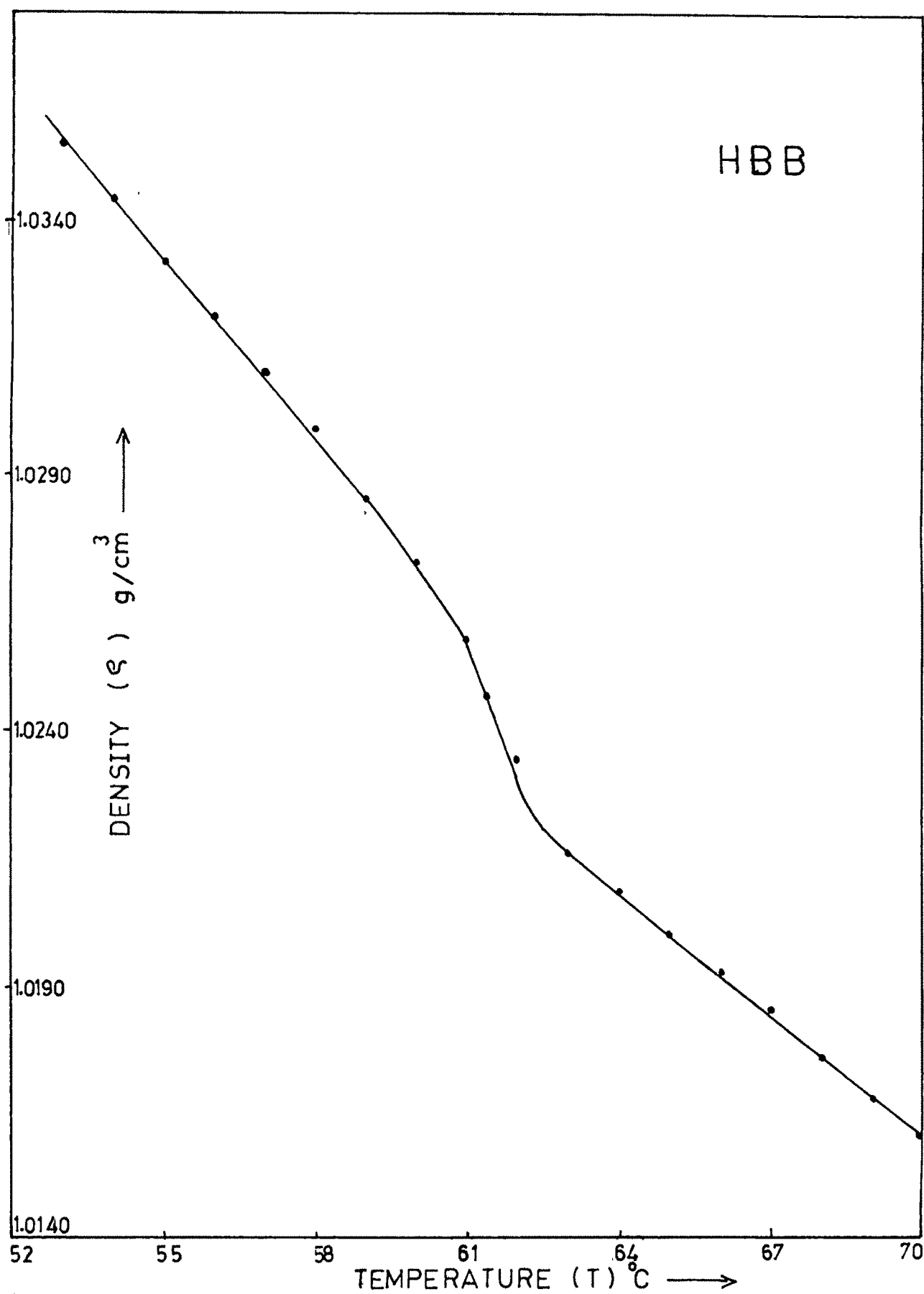


Figure A 14

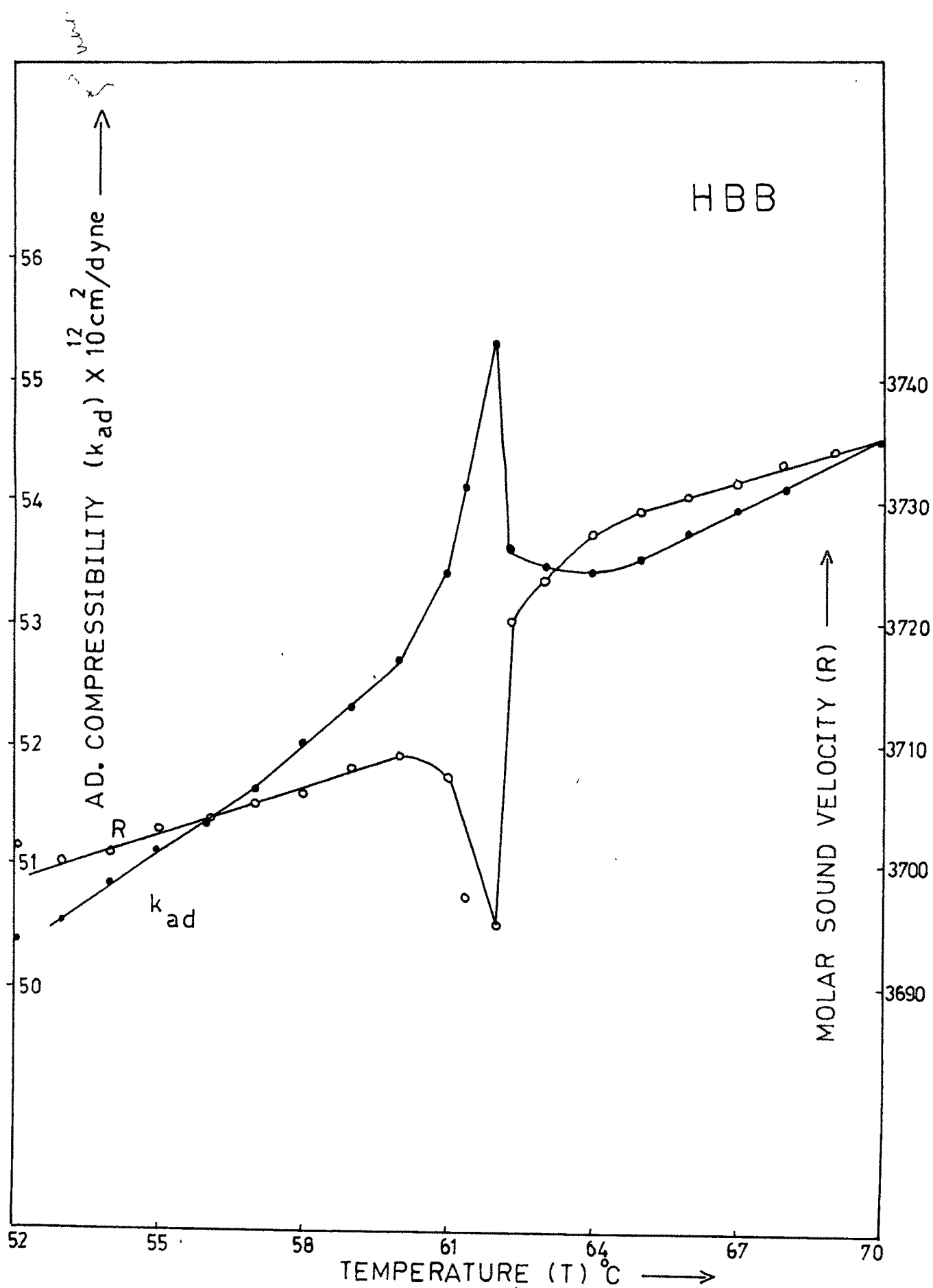
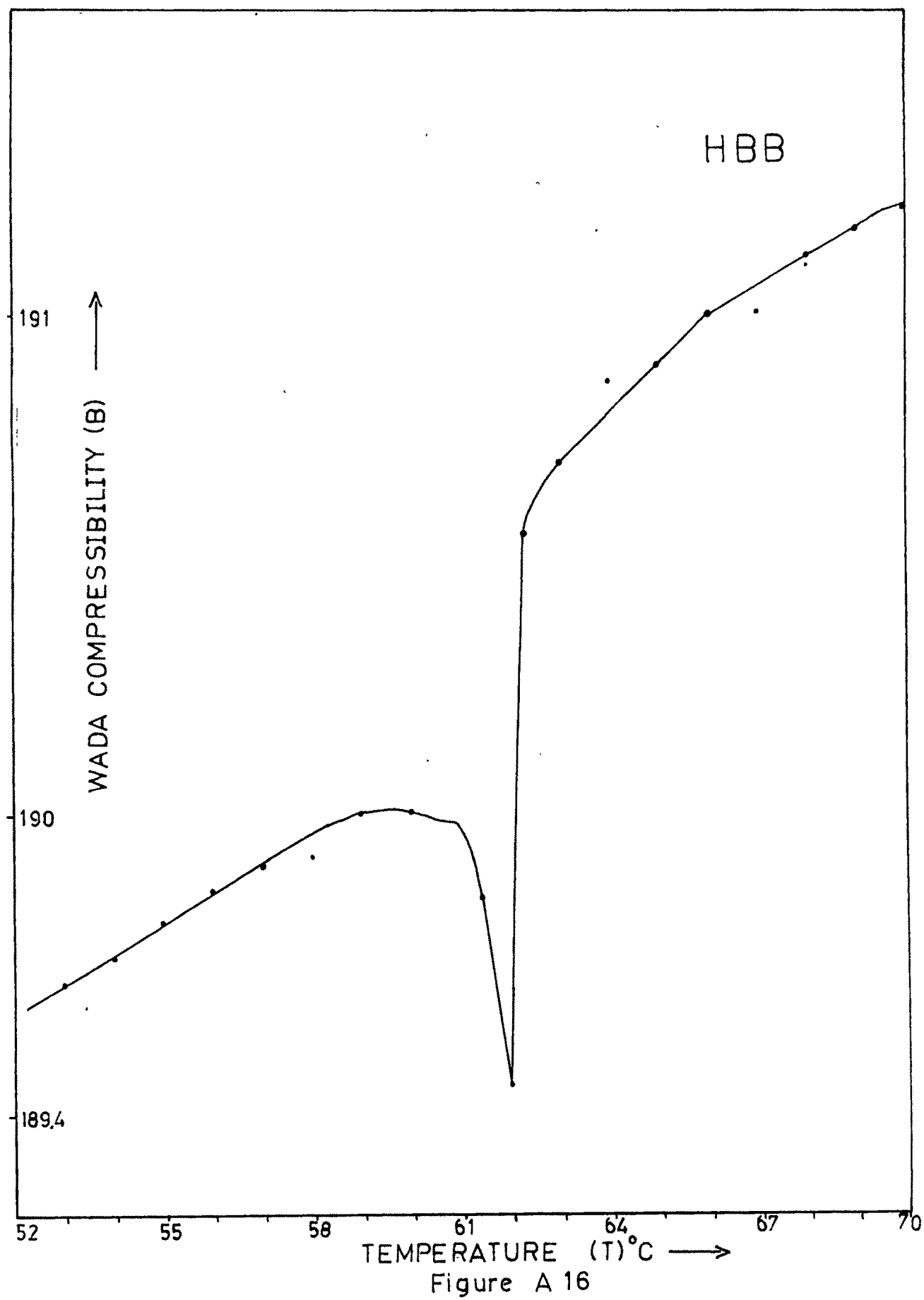


Figure A 15



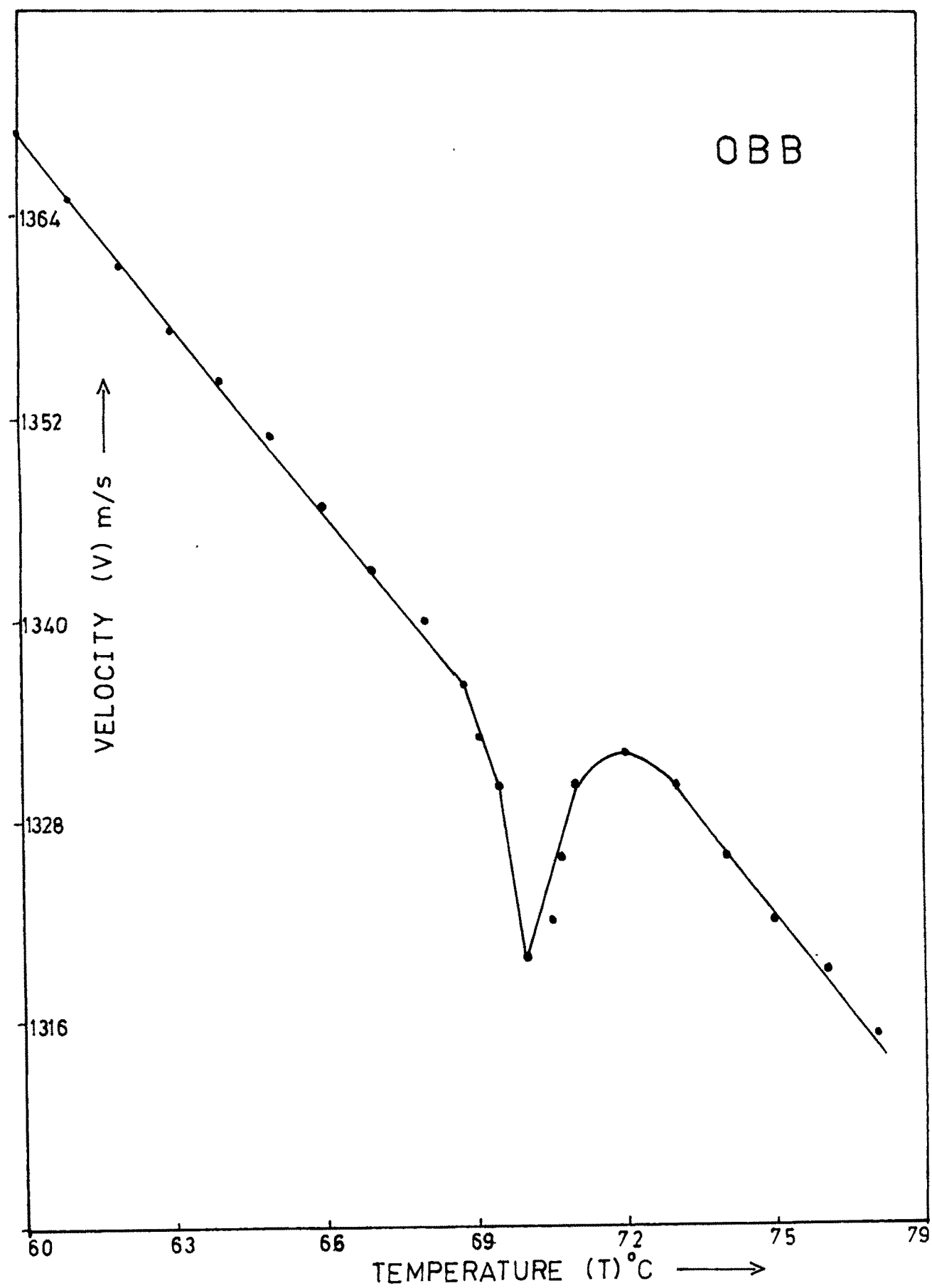


Figure A 17

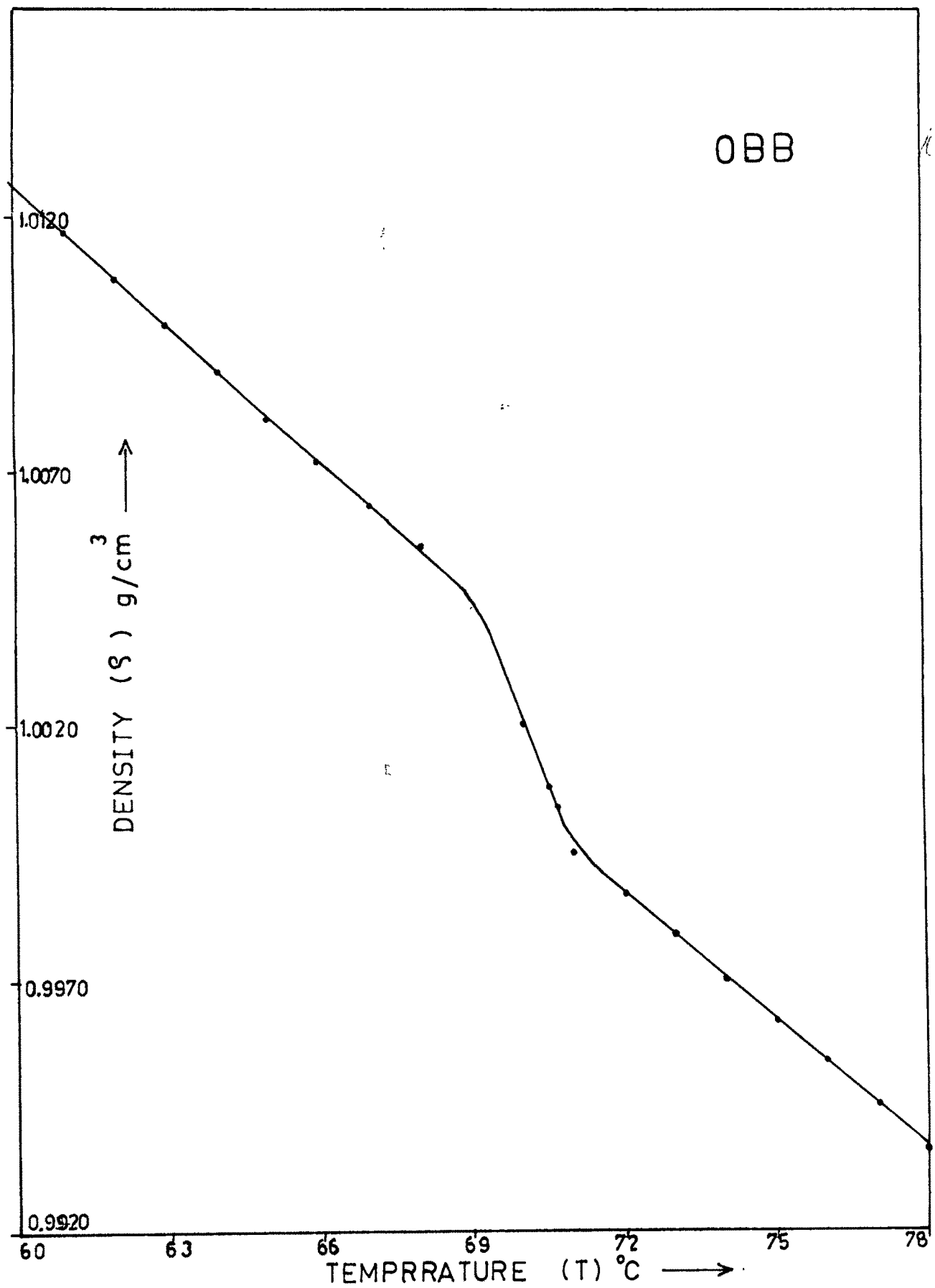


Figure A 18

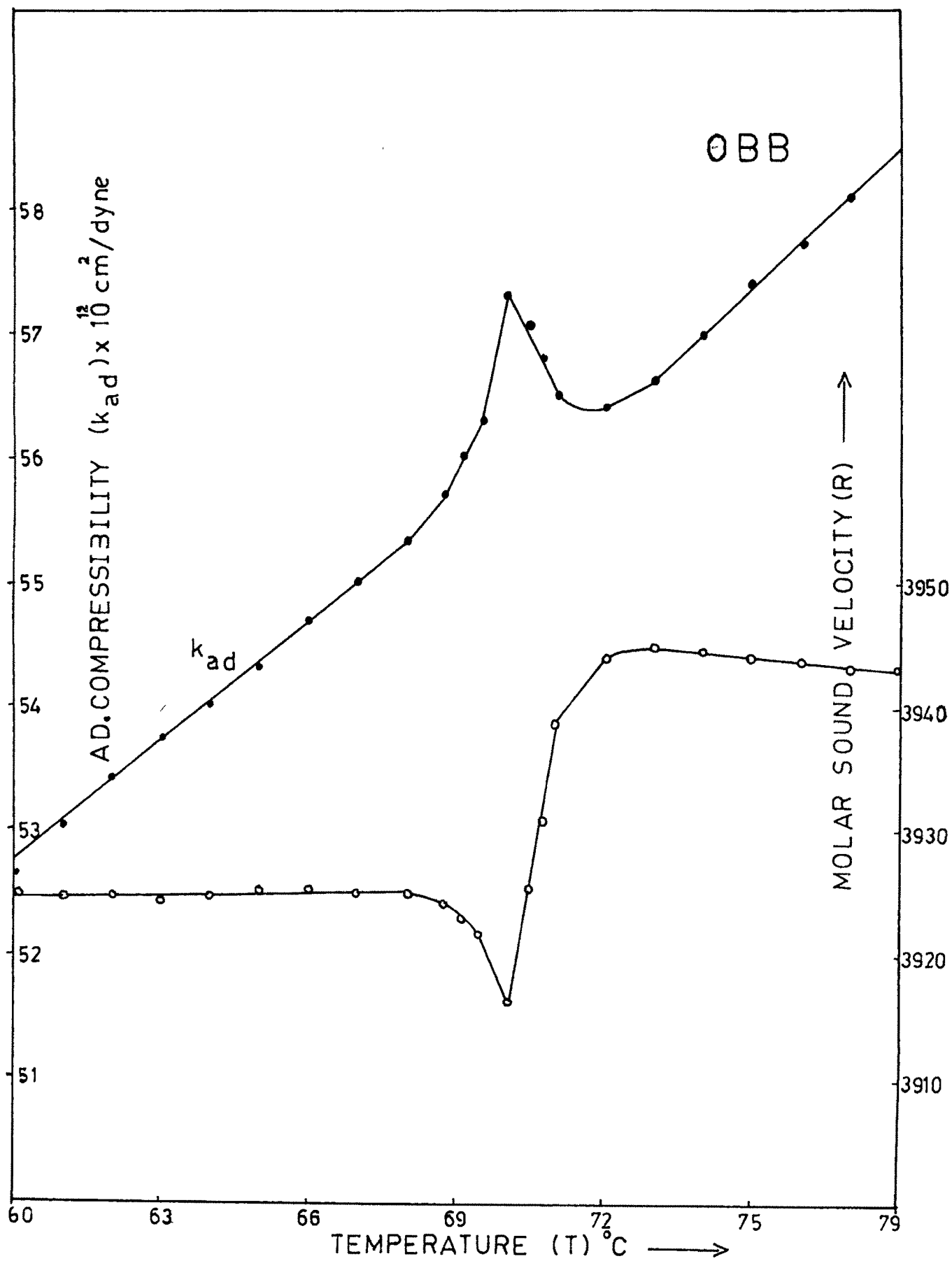


Figure A 19

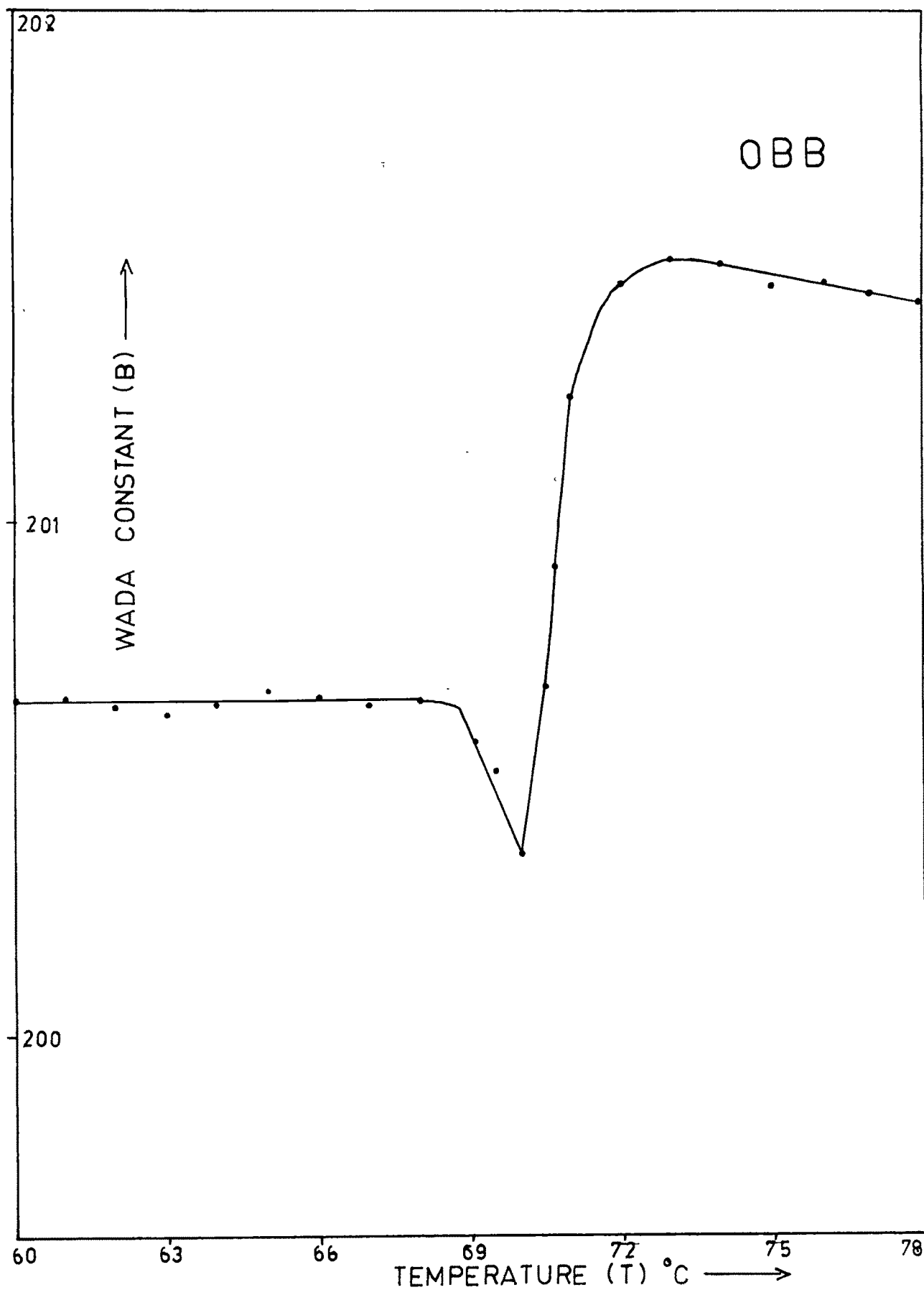


Figure A 20

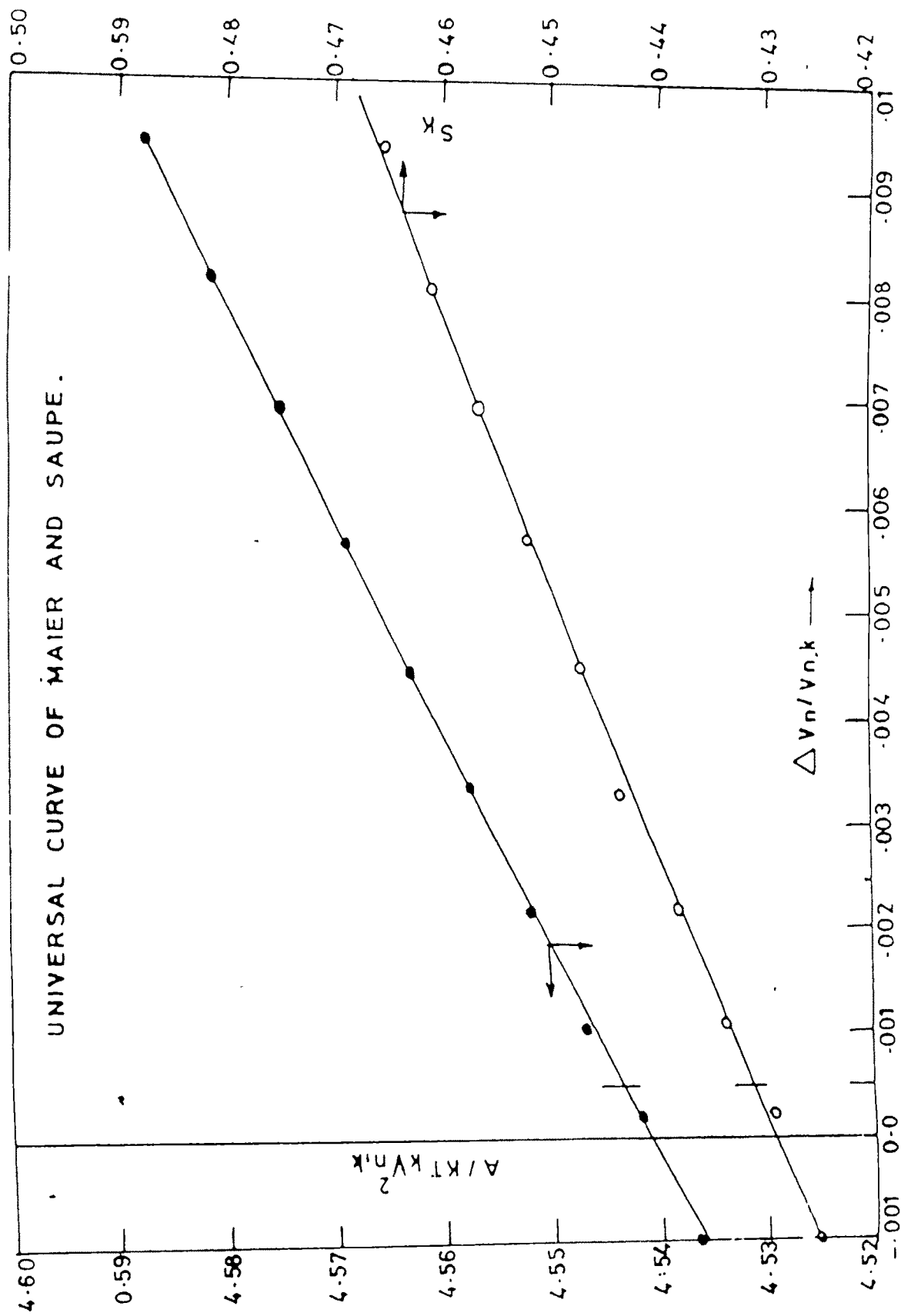


FIGURE - B

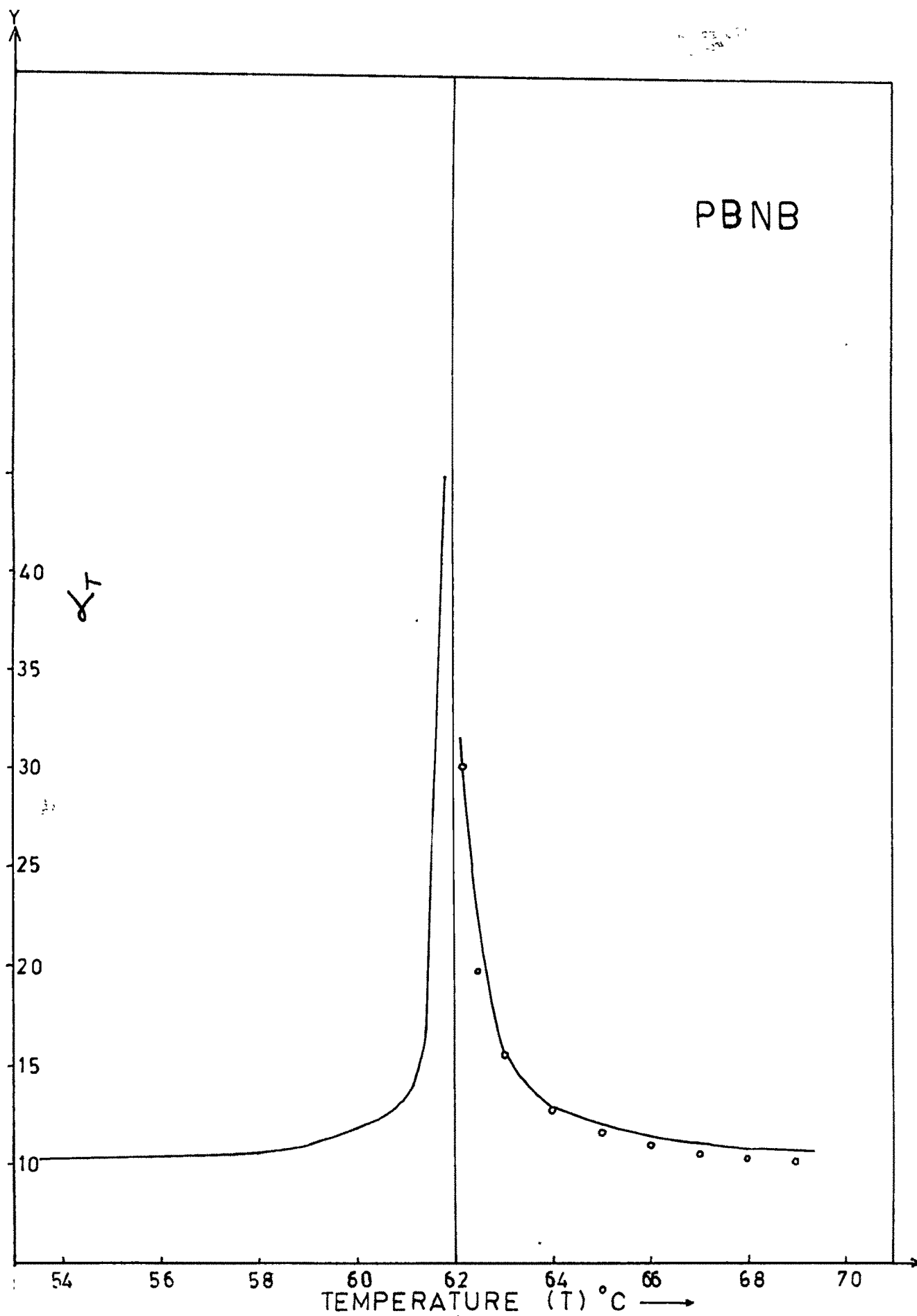


Figure B 1

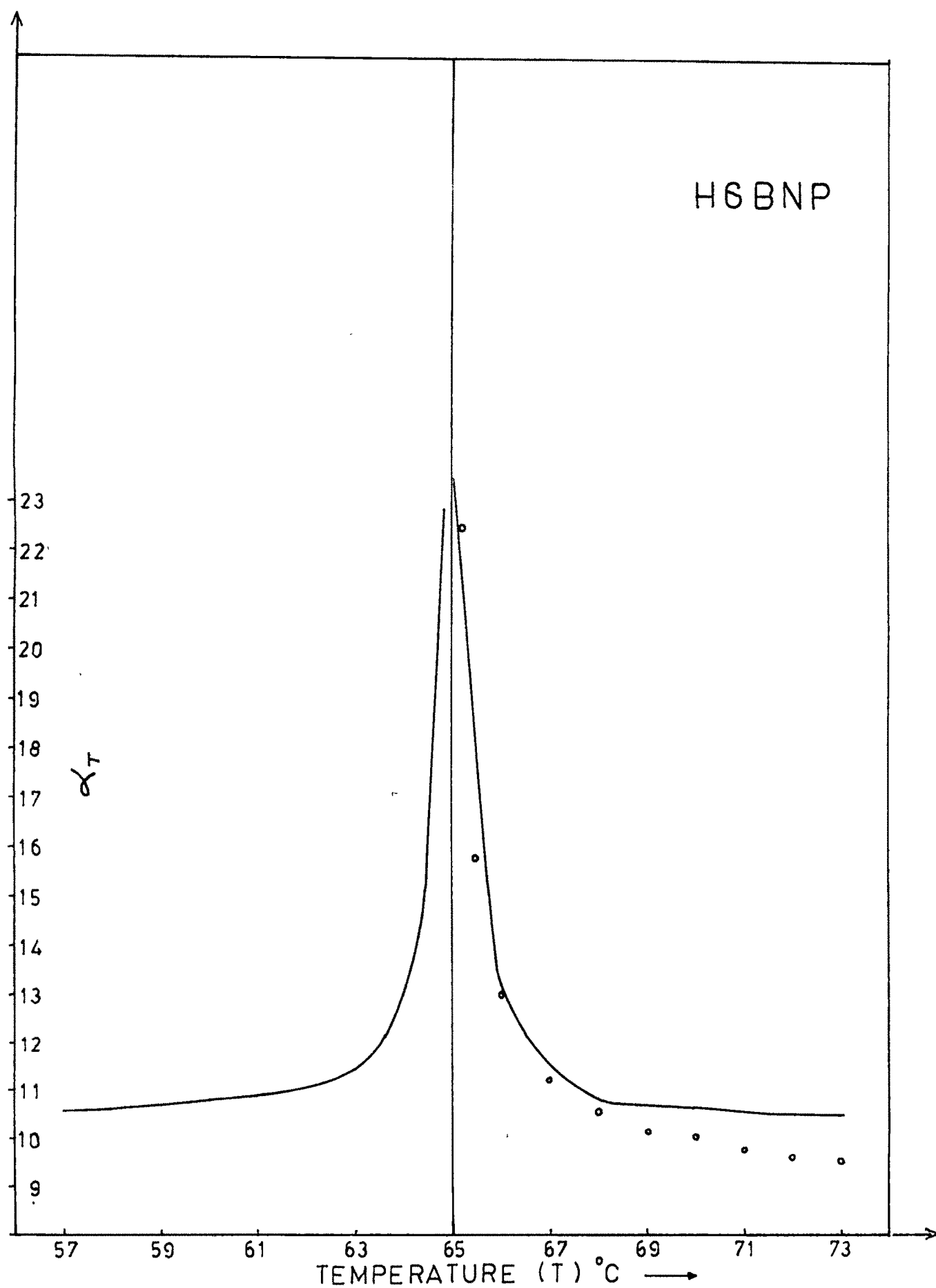


Figure B 2

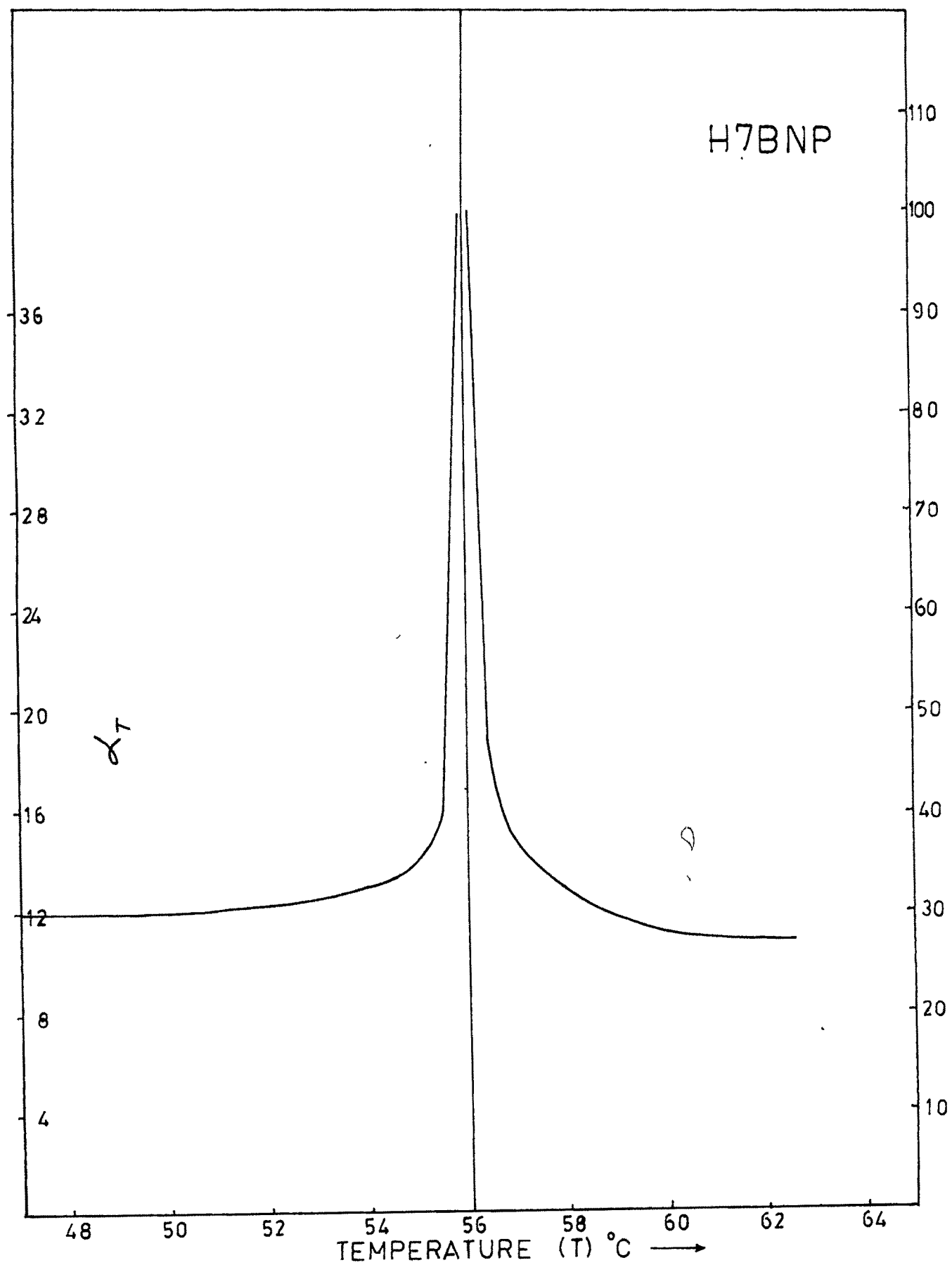


Figure B 3

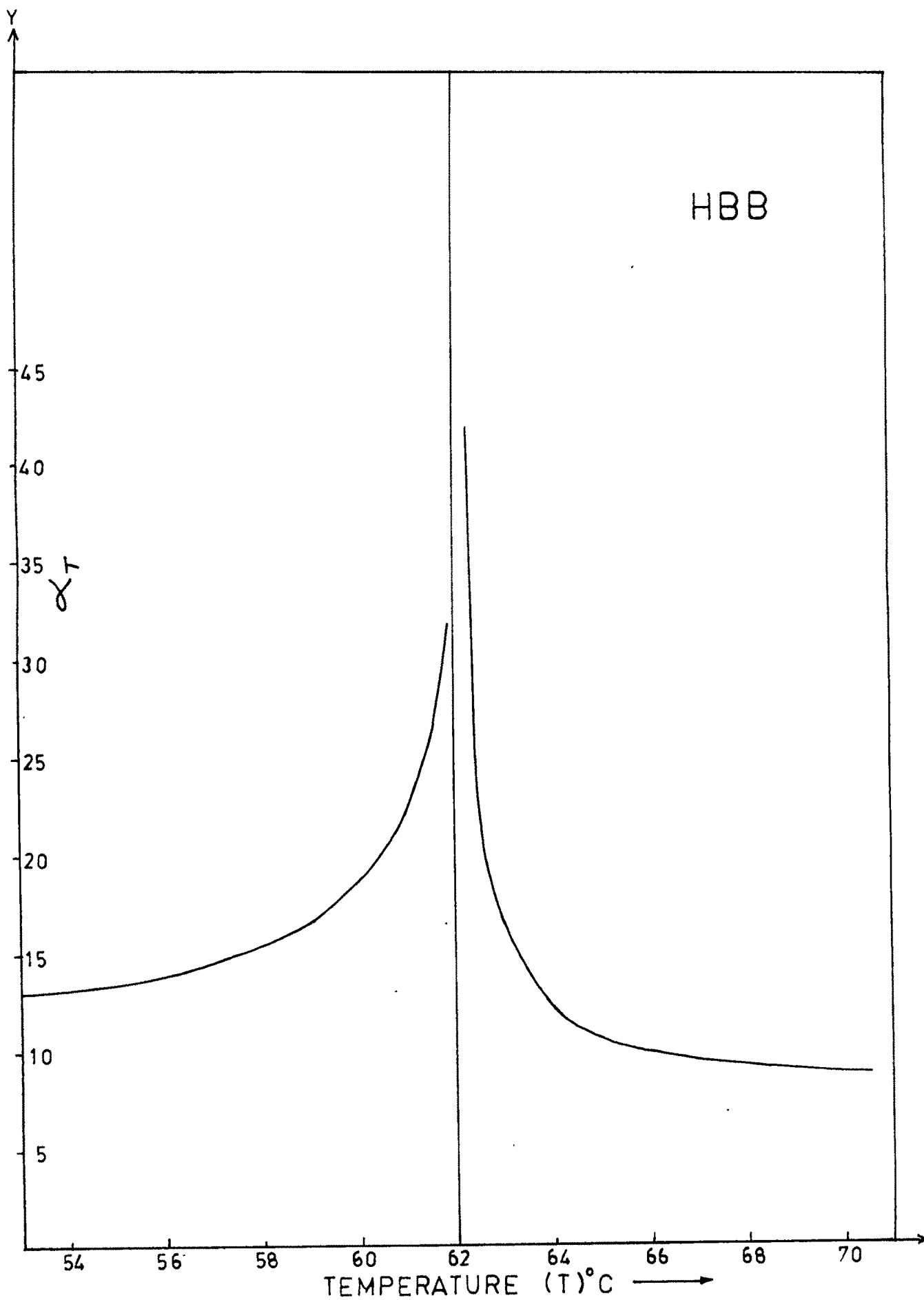


Figure B 4

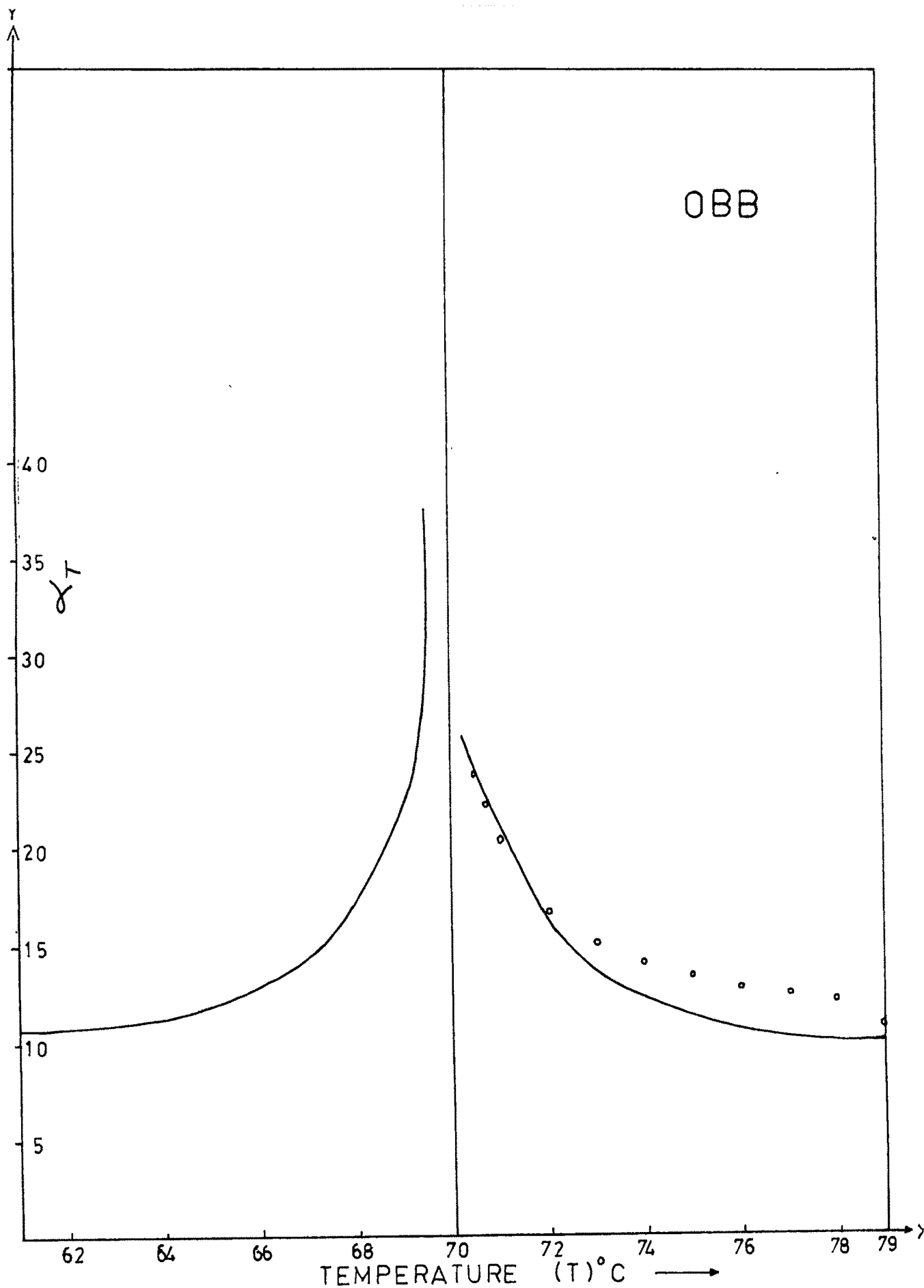


Figure B 5

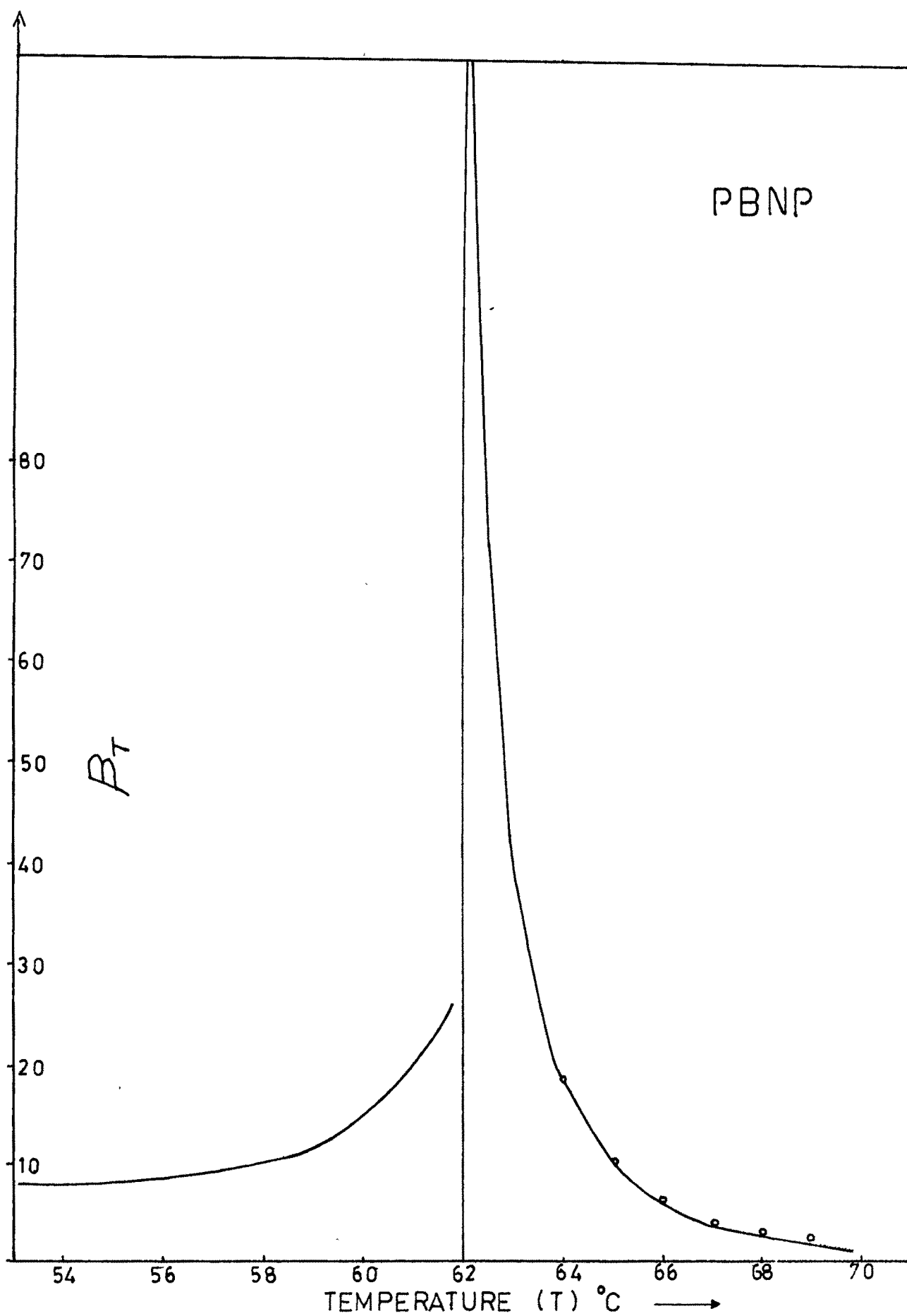


Figure B 6

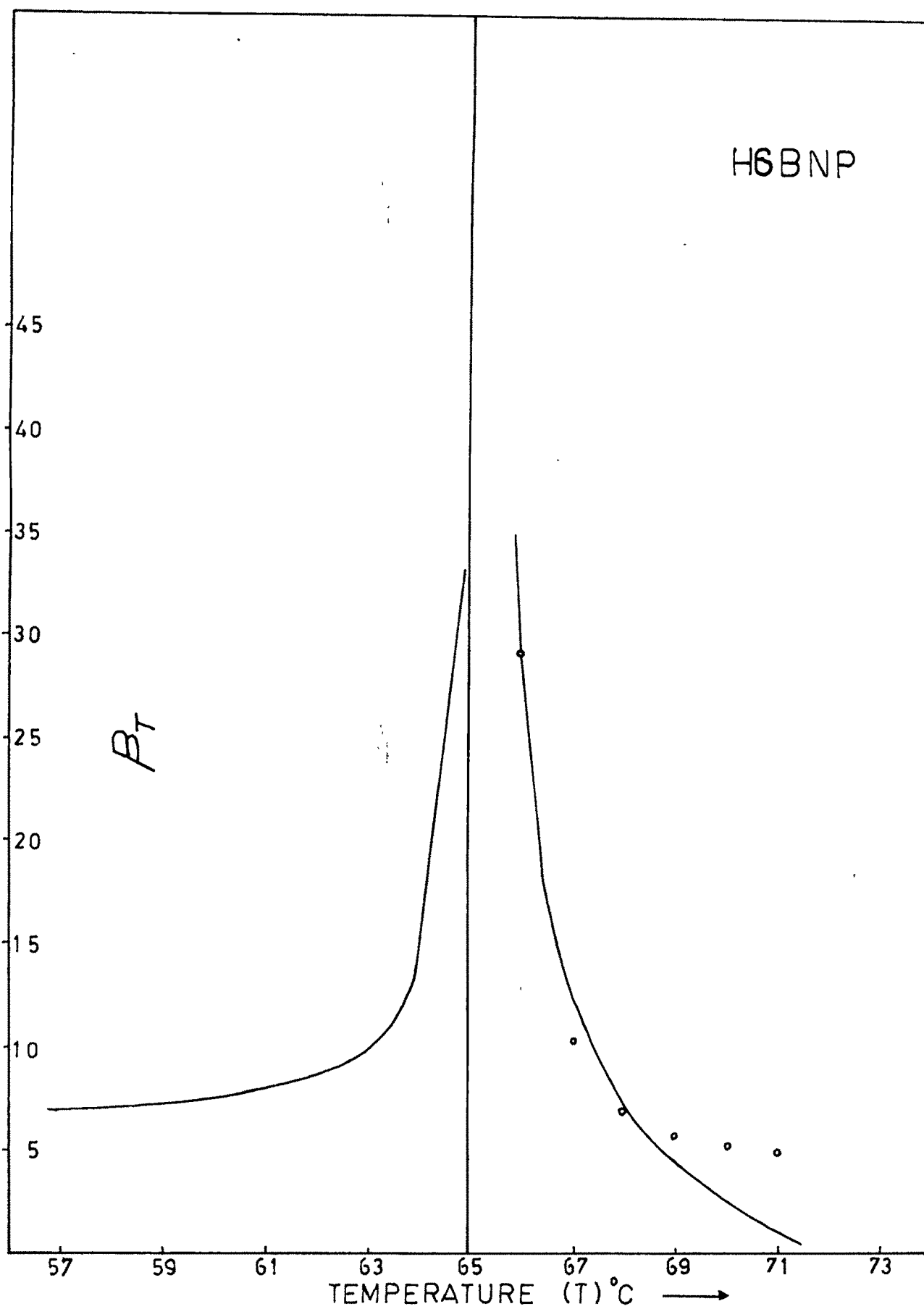


Figure B 7

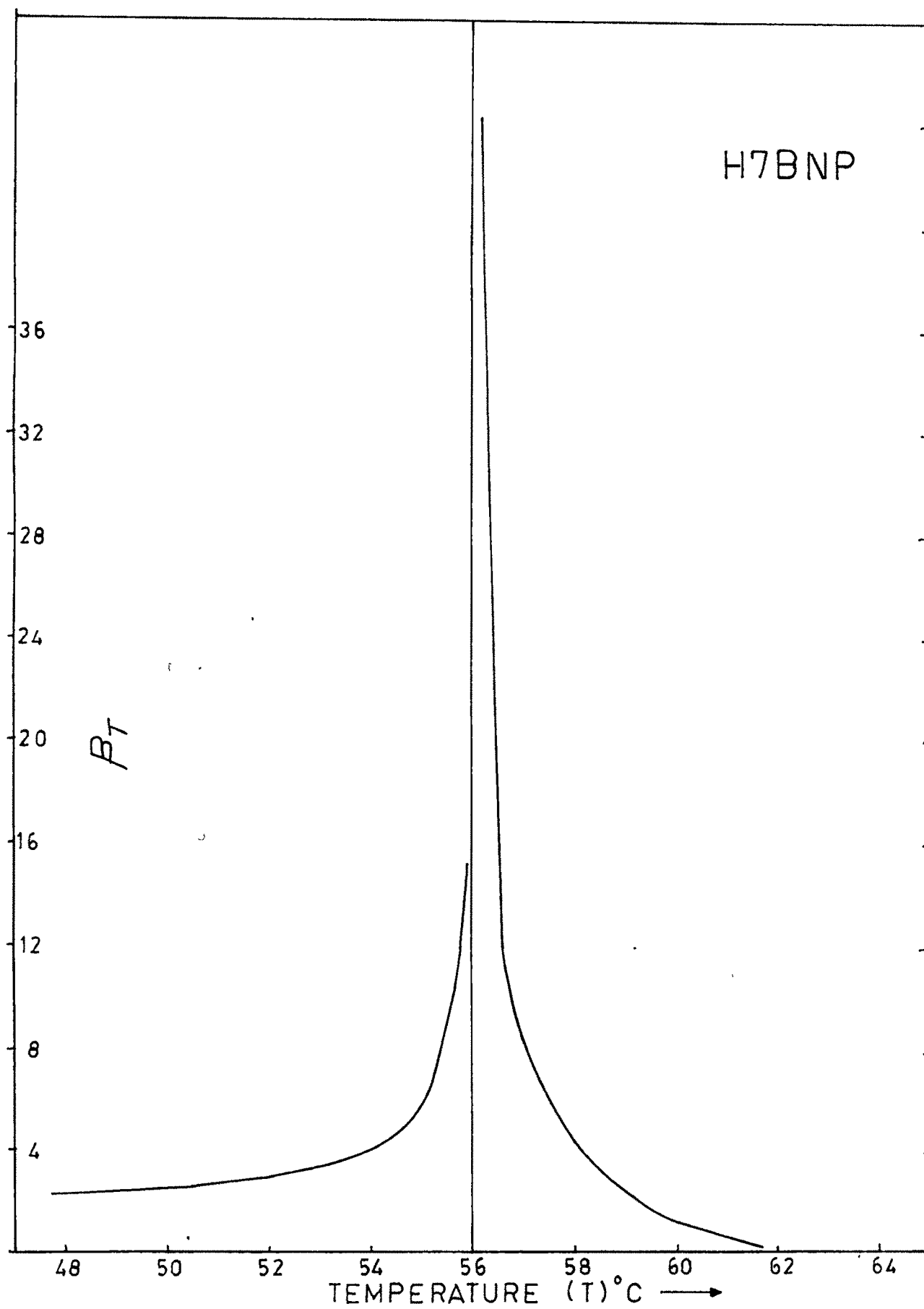


Figure B 8

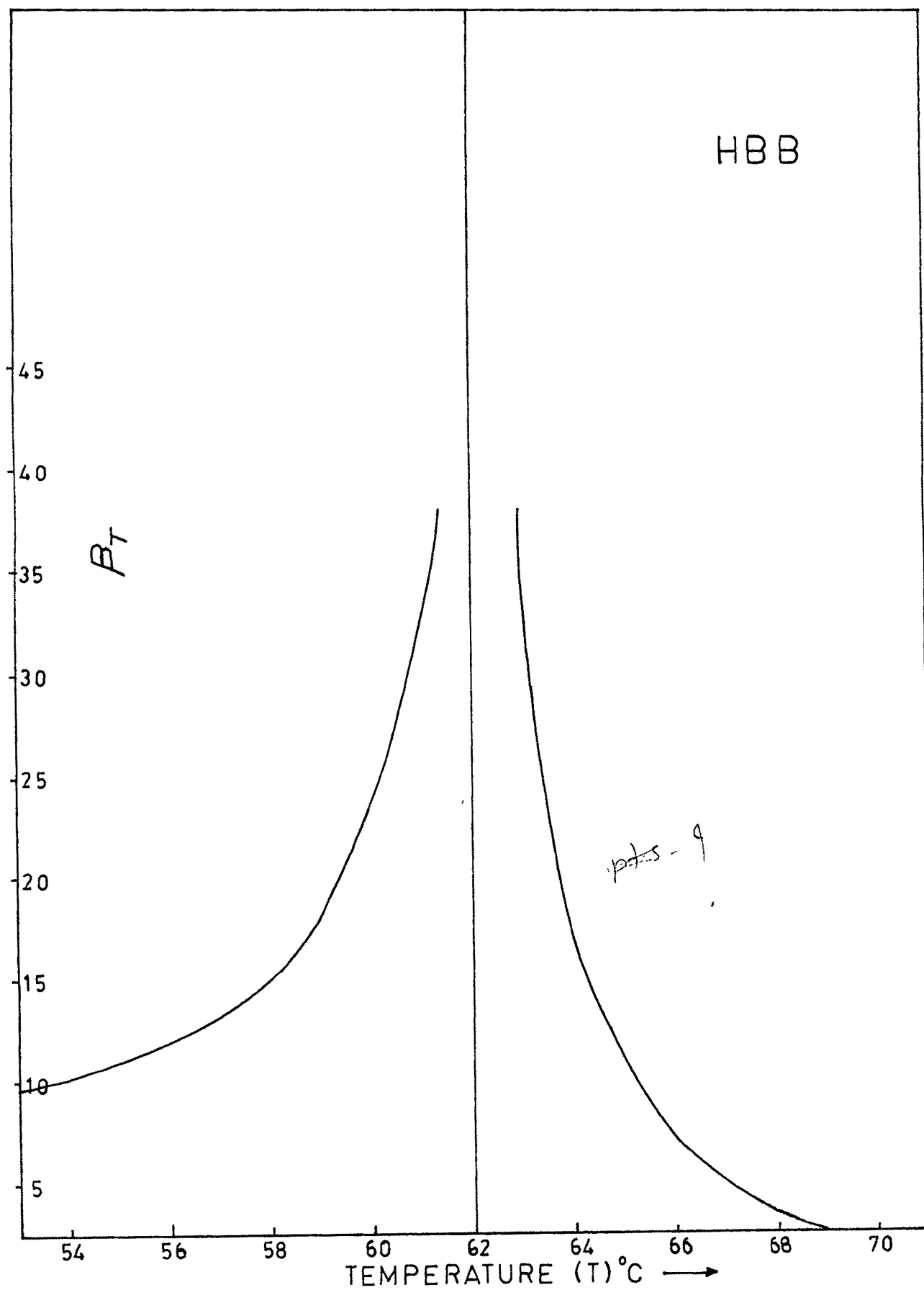


Figure B 9

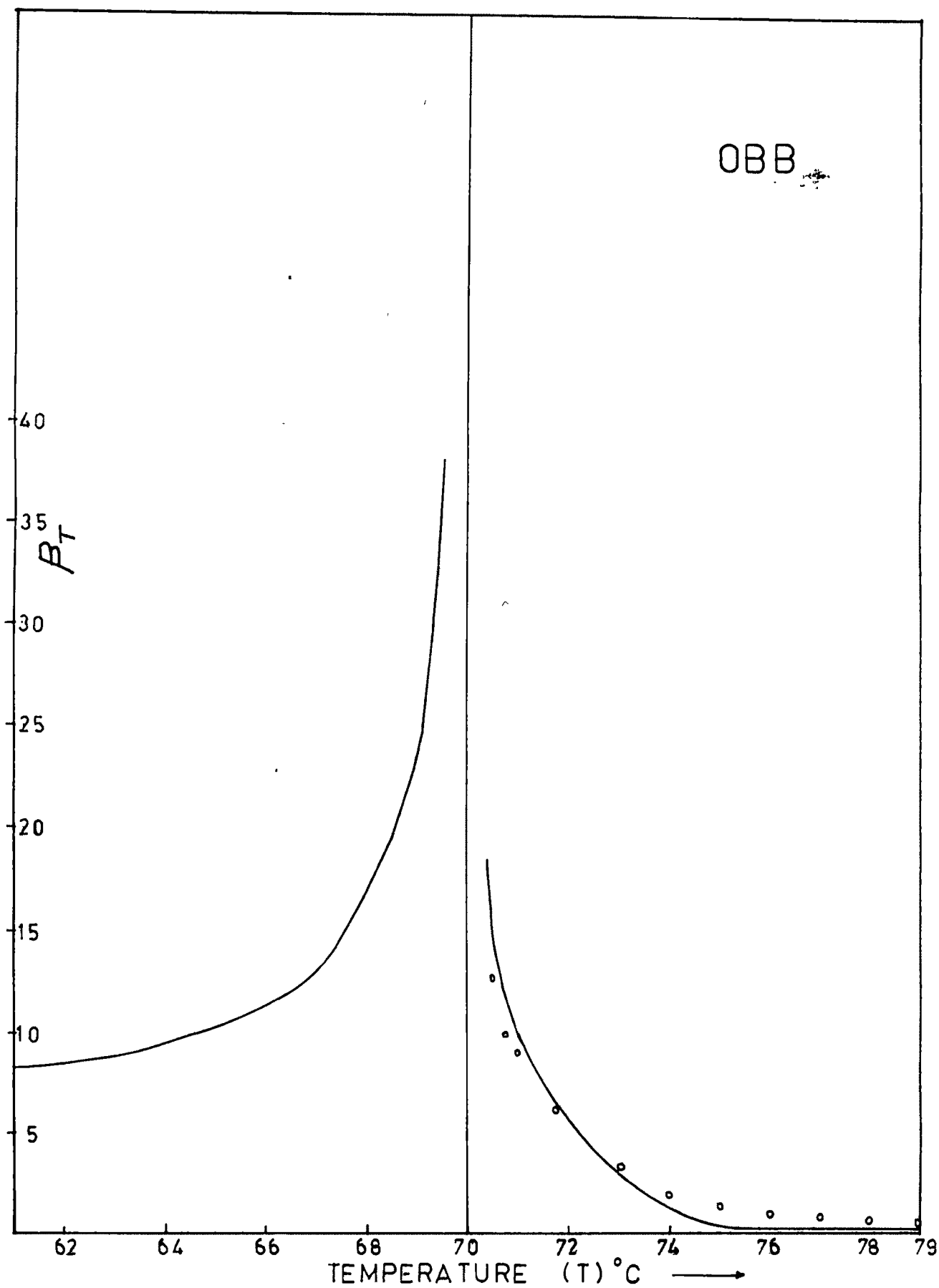


Figure B 10

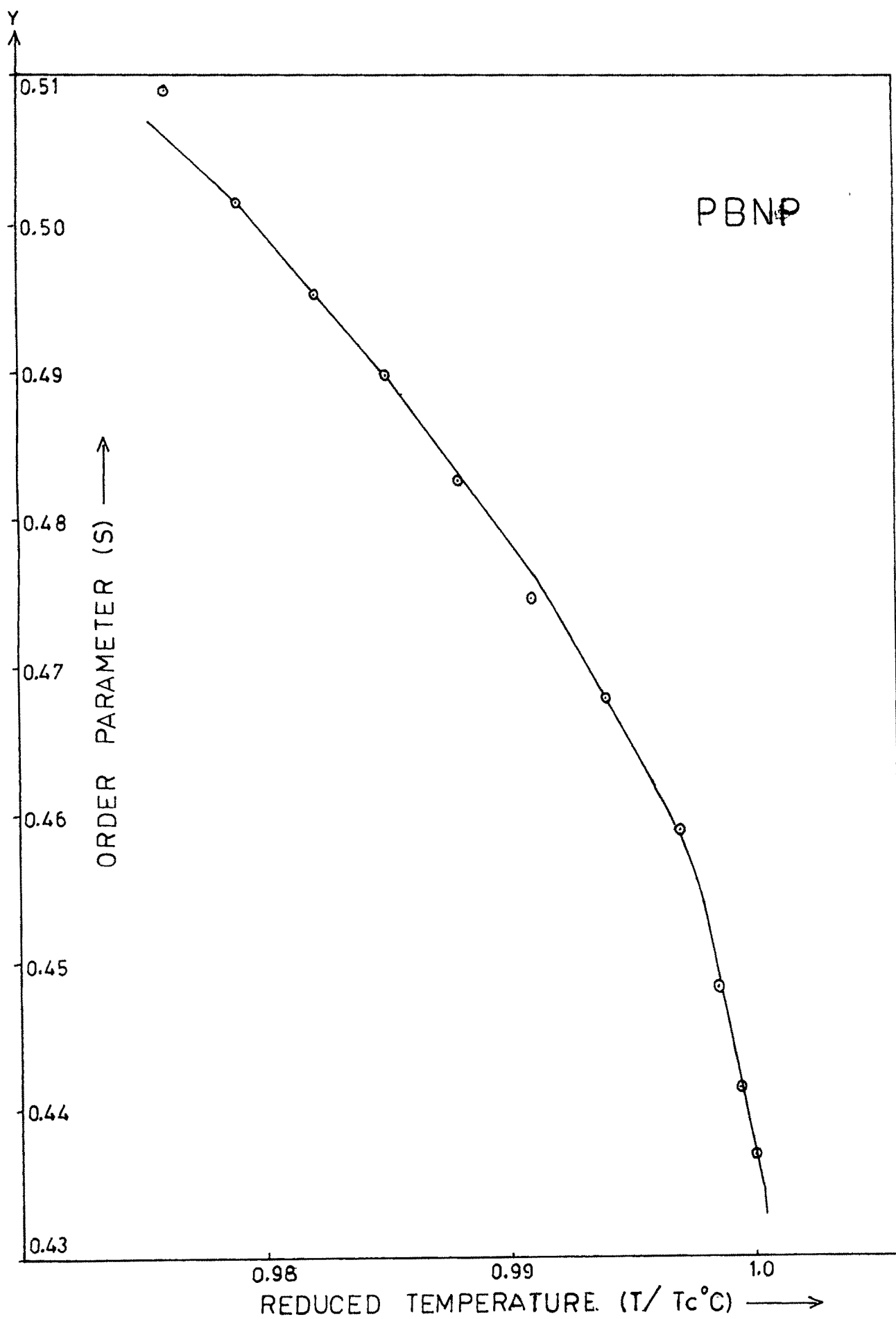


Figure B11

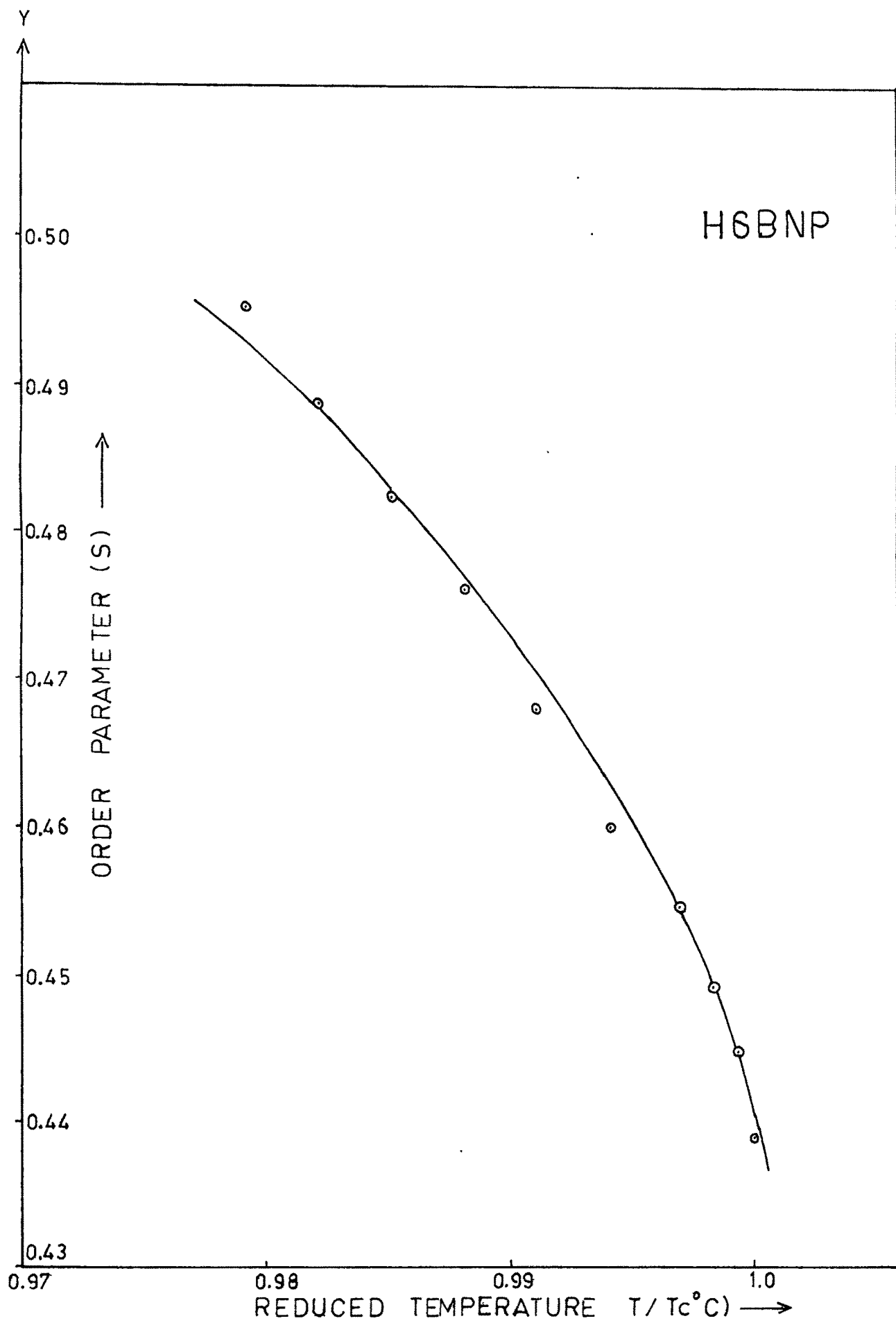


Figure B 12

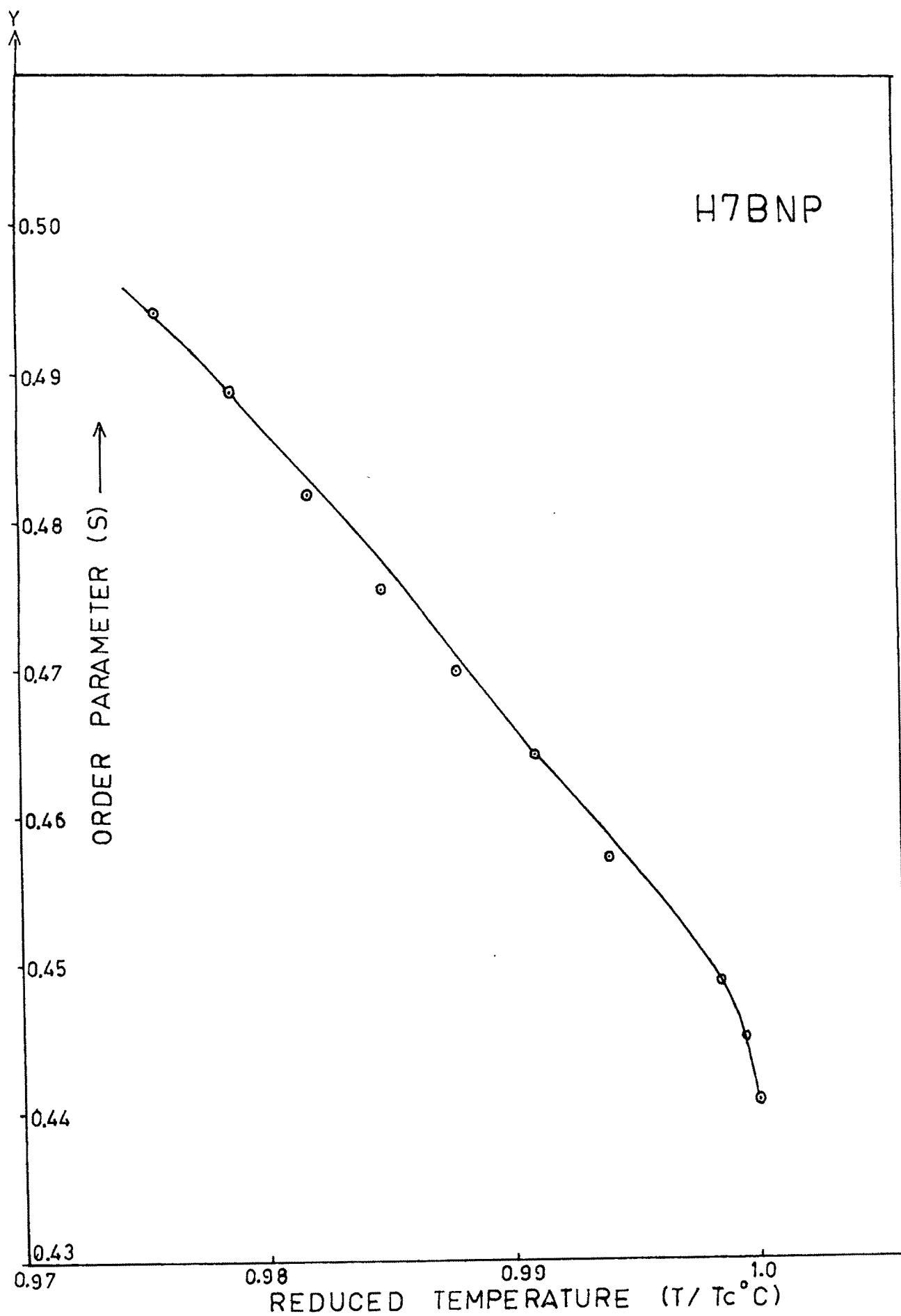


Figure B 13

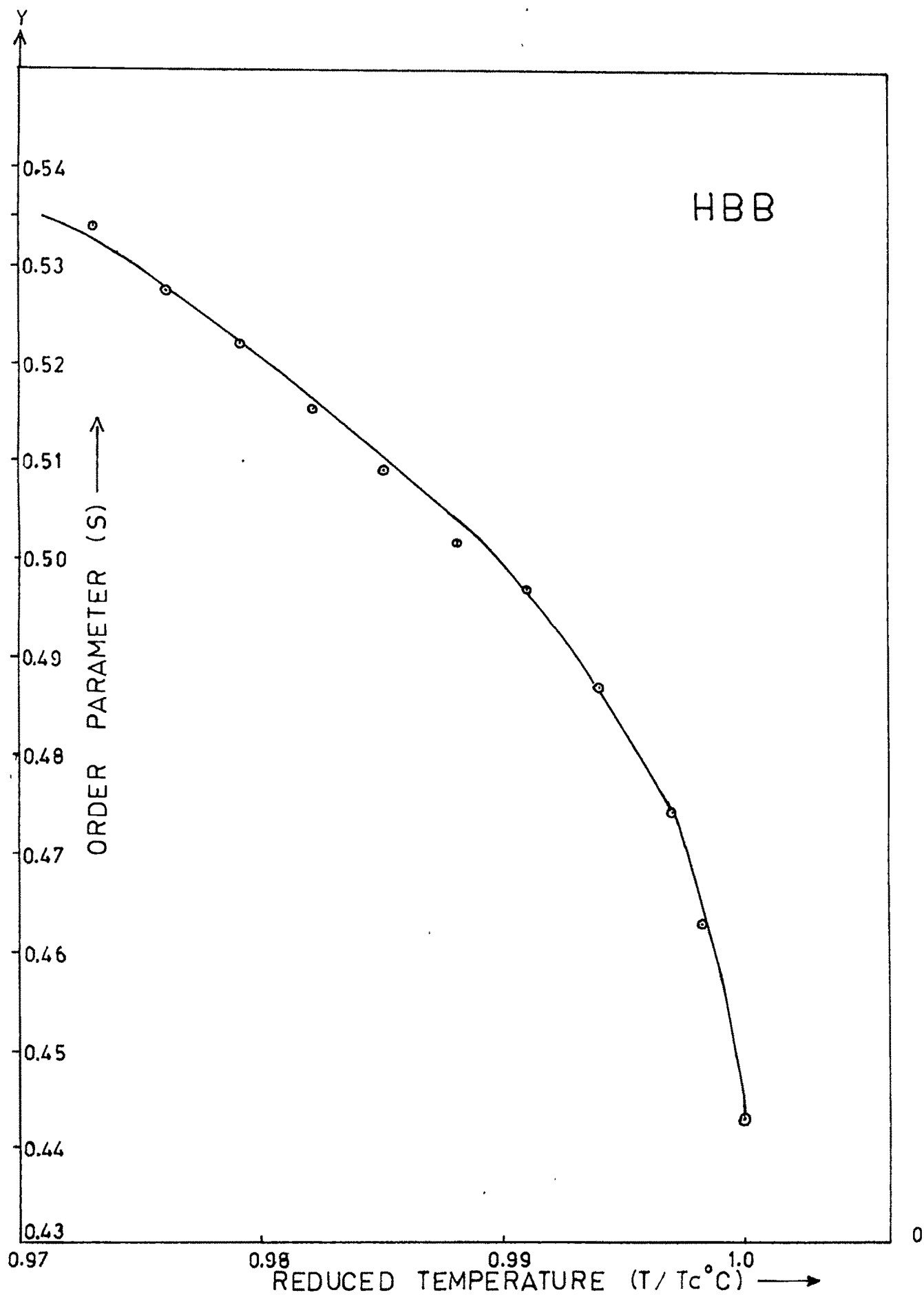


Figure B 14

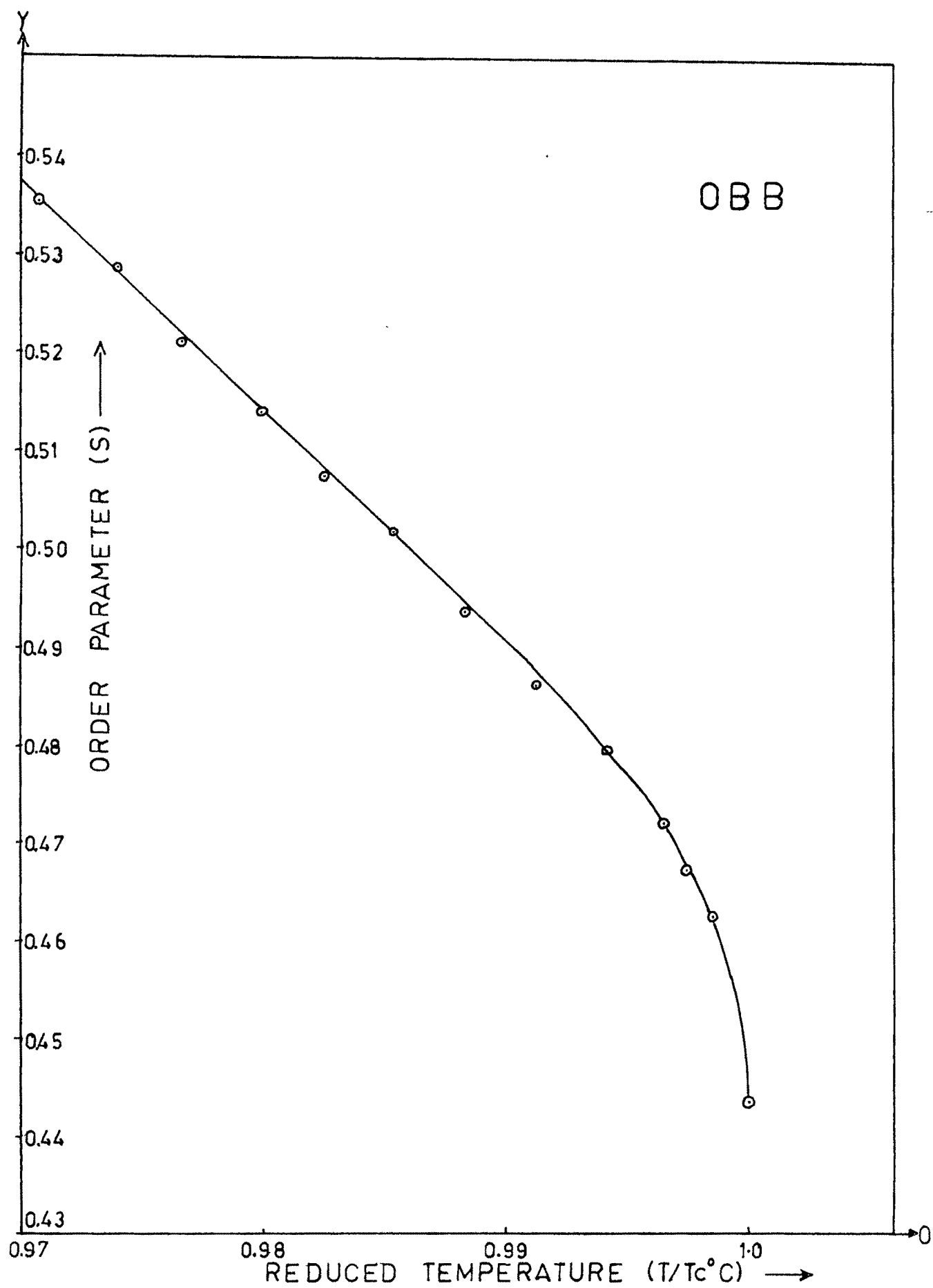


Figure B 15